



**HAL**  
open science

# Calcium, Acylation, and Molecular Confinement Favor Folding of *Bordetella pertussis* Adenylate Cyclase CyaA Toxin into a Monomeric and Cytotoxic Form

Johanna C. Karst, V. Yvette Ntsogo Enguéné, Sara E. Cannella, Orso Subrini, Audrey Hessel, Sylvain Debard, Daniel Ladant, Alexandre Chenal

► **To cite this version:**

Johanna C. Karst, V. Yvette Ntsogo Enguéné, Sara E. Cannella, Orso Subrini, Audrey Hessel, et al.. Calcium, Acylation, and Molecular Confinement Favor Folding of *Bordetella pertussis* Adenylate Cyclase CyaA Toxin into a Monomeric and Cytotoxic Form. *Journal of Biological Chemistry*, 2014, 289 (44), pp.30702-30716. 10.1074/jbc.M114.580852 . pasteur-01408931

**HAL Id: pasteur-01408931**

**<https://pasteur.hal.science/pasteur-01408931>**

Submitted on 5 Dec 2016

**HAL** is a multi-disciplinary open access archive for the deposit and dissemination of scientific research documents, whether they are published or not. The documents may come from teaching and research institutions in France or abroad, or from public or private research centers.

L'archive ouverte pluridisciplinaire **HAL**, est destinée au dépôt et à la diffusion de documents scientifiques de niveau recherche, publiés ou non, émanant des établissements d'enseignement et de recherche français ou étrangers, des laboratoires publics ou privés.



Distributed under a Creative Commons Attribution - NonCommercial - NoDerivatives 4.0 International License

Calcium, acylation and molecular confinement favor folding of *Bordetella pertussis* adenylate cyclase CyaA toxin into a monomeric and cytotoxic form.

Johanna C. Karst<sup>X</sup>, V. Yvette Ntsogo Enguéné<sup>X</sup>, Sara E. Cannella, Orso Subrini, Audrey Hessel, Sylvain Debard, Daniel Ladant\* and Alexandre Chenal\*

Institut Pasteur, CNRS UMR 3528, Unité de Biochimie des Interactions Macromoléculaires, Département de Biologie Structurale et Chimie, 28 rue du Dr Roux, 75724 Paris cedex 15, France.

Running title: Folding of CyaA into a monomeric and functional state

\* Corresponding authors: Alexandre Chenal, Unité de Biochimie des Interactions Macromoléculaires, CNRS URA 3528, Institut Pasteur, 28 rue du Dr. Roux, 75724 Paris cedex 15, France. Tel: 331 44 38 92 12; Fax: 331 40 61 30 42; email: [alexandre.chenal@pasteur.fr](mailto:alexandre.chenal@pasteur.fr); Daniel Ladant, Unité de Biochimie des Interactions Macromoléculaires, CNRS URA 3528, Institut Pasteur, 28 rue du Dr. Roux, 75724 Paris cedex 15, France. Tel: 331 45 68 84 00; Fax: 331 40 61 30 42; email: [daniel.ladant@pasteur.fr](mailto:daniel.ladant@pasteur.fr)

<sup>X</sup>: These authors contributed equally

Keywords: adenylate cyclase (adenylyl cyclase); bacterial toxin; *Bordetella pertussis*; calcium-binding protein; chromatography; macromolecular crowding; protein acylation; protein aggregation; protein folding; molecular confinement

**Background:** Due to its hydrophobic character, the adenylate cyclase (CyaA) toxin from *Bordetella pertussis* is prone to aggregate into multimeric forms.

**Results:** We define the experimental conditions to fold CyaA into a monomeric state.

**Conclusion:** Molecular confinement, post-translational acylation and calcium binding are critical for CyaA folding into a monomeric and cytotoxic form.

**Significance:** Monomeric CyaA opens the way for structural and functional studies.

## ABSTRACT

The adenylate cyclase (CyaA) toxin, a multidomain protein of 1706 amino-acids, is one of the major virulence factors produced by *Bordetella pertussis*, the causative agent of whooping cough. CyaA is able to invade eukaryotic target cells in which it produces high levels of cAMP thus altering the cellular physiology. Although CyaA has been extensively studied by various cellular and molecular approaches, the structural and functional states of the toxin remain poorly

characterized. Indeed, CyaA is a large protein and exhibits a pronounced hydrophobic character making it prone to aggregation into multimeric forms. As a result, CyaA has been usually extracted and stored in denaturing conditions. Here, we define the experimental conditions allowing CyaA folding into a monomeric and functional species. We found that CyaA forms mainly multimers when refolded by dialysis, dilution or buffer exchange. However, a significant fraction of monomeric, folded protein could be obtained by exploiting molecular confinement on size-exclusion chromatography. Folding of CyaA into a monomeric form was found to be critically dependent upon the presence of calcium and post-translational acylation of the protein. We further show that the monomeric preparation displayed hemolytic and cytotoxic activities suggesting the monomer is the genuine, physiologically active form of the toxin. We hypothesize that the structural role of the post-translational acylation in CyaA folding may apply to other RTX toxins.

**Introduction.** The adenylate cyclase (CyaA) toxin produced by *Bordetella pertussis*, the causative agent of whooping cough, is one of the major virulence factors of this organism (1-3). CyaA plays an important role in the early stages of respiratory tract colonization by *B. pertussis*. CyaA is able to invade eukaryotic target cells, where it is activated by an endogenous protein, calmodulin (CaM), and produces high levels of cAMP that, in turn, alters the cellular physiology.

CyaA is a 1706-residue long protein organized in a modular fashion (Figure 1A). The ATP-cyclizing, CaM-activated, catalytic domain (ACD) is located in the 400 amino-terminal residues (4) while the carboxy-terminal 1306 residues are responsible for the ACD translocation and the hemolytic phenotype of *B. pertussis* (5-7). Both activities can function independently as adenylate cyclase and haemolysin, respectively. Several domains can be identified in the C-terminal region. The so-called translocation region, spanning residues 400 to 500, is crucial for the translocation of ACD across the plasma membrane (8) and exhibits properties related to membrane-active peptides (9). The hydrophobic region, spanning residues 500 to 750, contains several hydrophobic segments predicted to adopt alpha-helical structures. The acylation region, spanning residues 800 to 1000, contains two post-translational modification sites that are essential for the cytotoxic activities of CyaA (10-12). The toxin is indeed synthesized as an inactive precursor, proCyaA that is converted into the active CyaA toxin upon specific acylation of Lys 860 and Lys 983 by a dedicated acyltransferase, CyaC (10,11,13). The C-terminal part of CyaA is the cell receptor-binding domain (RD, residues 1000 to 1706). This domain consists of ~40 copies of a calcium-binding, glycine and aspartate-rich nonapeptide repeat that is characteristic of a large family of bacterial cytolysins known as RTX (Repeat-in-ToXin) toxins (14,15). These motifs constitute the main Ca<sup>2+</sup> binding sites of the protein (16). The RTX motifs are intrinsically disordered in the absence of calcium (17-20). The intrinsic disorder predictors ((21-24) Figure 1B-D) show that RD

is characterized by structural disorder and a significant negative mean net charge, which is partially neutralized upon calcium binding, as experimentally reported elsewhere (25). In the presence of calcium, RTX proteins fold into a structure called  $\beta$ -roll as revealed in the three-dimensional structures of several RTX proteins (26-28). CyaA is secreted across the bacterial envelope by a dedicated type I secretion machinery (29) made of CyaB, CyaD, and CyaE proteins (5,30). Once secreted, CyaA binds in a calcium-dependent manner to the CD11b/CD18 integrin expressed on myeloid cells, such as macrophages, neutrophils, dendritic cells, and natural killer cells that are the primary targets of this toxin *in vivo* (31). Yet, CyaA can also efficiently intoxicate a variety of cell types lacking this receptor (16,32-35).

One of the main originalities of CyaA, with respect to other bacterial or plant toxins, stems from its unique mechanism of penetration into eukaryotic cells: CyaA is the only known toxin able to translocate its catalytic domain directly across the plasma membrane of the target cells, from the extra-cellular side into the cytosol (36-41). The molecular mechanism by which CyaA enters the target cells remains, however, largely unknown. It is believed that after binding via the RD domain to the CD11b/CD18 receptor, the hydrophobic regions of CyaA may insert into the plasma membrane of the target cells. The catalytic domain is then delivered through the plasma membrane, possibly through a transient and local destabilization of the membrane integrity (8,9,42,43) to reach the cytosol, where upon binding to the endogenous CaM, its enzymatic activity is stimulated to generate supra physiologic levels of cAMP (37,44). Moreover, CyaA, after insertion into the membrane, can also form cation-selective pores, which impair membrane impermeability and ultimately cause cell lysis (6,40,45). This membrane damaging activity is thought to synergize with the cAMP intoxication ability thus increasing the overall cytotoxicity of the toxin (33,40,46,47).

Although CyaA has been extensively studied by various cellular and molecular approaches and used in several biotechnological applications, the structural and functional states

of the toxin remain poorly characterized (1,2). Indeed, CyaA is a large protein made of several distinct domains and exhibits a pronounced hydrophobic character, making it prone to aggregation into multimeric complexes (37,48-50). Up to now, CyaA has been mainly extracted from *B. pertussis* with a chaotropic reagent (urea) or overproduced in *E. coli* where it accumulates as inclusion bodies that also need to be solubilized with urea. After purification CyaA is usually stored in denaturing conditions, typically in the presence of 6 M urea (37,48,51-53).

Here, we defined the experimental conditions to refold CyaA into a monomeric and functional species. We found that CyaA, when refolded by dialysis, dilution or buffer exchange, mainly produced multimers, as reported earlier (37,48). However, by exploiting molecular confinement on size-exclusion chromatography (SEC), we were able to obtain a monomeric form of CyaA that was stable in buffer without urea. Noticeably, this monomeric form exhibited much higher hemolytic and cell-invasive activities than the multimeric ones. CyaA refolding into the monomeric state was critically dependent upon the presence of calcium and the post-translational acylation. The structural role of both calcium and acyl chains in CyaA folding demonstrated here may possibly apply to other RTX cytolysins that are activated by selective acylation and dependent upon calcium for their cytolytic activities.

## Experimental procedures

### *CyaA production and purification*

CyaA was produced and purified from inclusion bodies as previously described (53,54). Briefly, the inclusion bodies were solubilized in about 50 ml of 20 mM Hepes, 8 M urea, pH 7.4, by overnight solubilization under constant stirring with a magnet at 4 °C. After centrifugation at 12000 rpm for 20 min, the supernatant was supplemented with 0.14 M NaCl and incubated for 1 hour at room temperature with 75 ml of Q-Sepharose resin equilibrated with 20 mM Hepes, 140 mM NaCl, 8 M urea, pH 7.4. The resin, retaining the CyaA protein, was then loaded onto a column and contaminants were washed out. After an extensive wash with the same buffer,

the CyaA protein was eluted in 20 mM Hepes, 500 mM NaCl, 8 M urea, pH 7.4. The eluate was then diluted in 20 mM Hepes, 8M urea to decrease salt down to 140 mM NaCl and loaded onto a second Q-sepharose column (50 mL). Washing and elution were performed in the same conditions as described above with the first Q media. This last step further removed contaminants and concentrated the CyaA protein. Proteins eluted from the second Q-sepharose column were diluted five times with 20 mM Hepes, 1 M NaCl, pH 7.4, and applied onto a 70-ml phenyl-sepharose column equilibrated with the same buffer. Resin was washed with 20 mM Hepes, 1 M NaCl, with Hepes 20 mM and then with 50 % isopropanol. The isopropanol washing step allowed the removal of many contaminants and LPS. After an extensive wash with 20 mM Hepes, the toxin was eluted with Hepes 20 mM, urea 8 M. The eluate was finally loaded onto a sephacryl 500 (*GE Healthcare, HIPREP 26/60*) equilibrated in 20 mM Hepes, 8 M urea. CyaA was then concentrated by ultrafiltration to 1-2 mg/ml and stored at -20°C in 20 mM Hepes, 8 M urea. All toxins purified by this method were more than 90% pure as judged by SDS PAGE analysis and contained less than 1 EU of LPS/μg of protein as determined by a standard LAL assay (Lonza). CyaA toxin concentrations were determined spectrophotometrically using a molecular extinction coefficient of 144 000 M<sup>-1</sup> cm<sup>-1</sup> at 280 nm. Altogether, the overall recovery from a 1.6-liter fermentor varies from 20 to 40 mg of pure CyaA proteins.

### *Refolding of urea-denatured CyaA*

The renaturation of CyaA from its denatured state in 8 M urea, was followed by tryptophan intrinsic fluorescence, ANS fluorescence and circular dichroism in the far-UV ranges at 25°C. Tryptophan intrinsic fluorescence was used to follow the changes of tryptophan environment, ANS fluorescence was used to follow the changes of hydrophobic environment (55) while ellipticity changes at 220 nm was used to follow secondary structural changes (19).

### *Intrinsic disorder predictions*

The primary sequence of CyaA was used to analysis the intrinsic structural disorder. The disorder predictions were first check with

MeDor (24), and the results present herein were obtained with GlobPlot, IUPred and FoldIndex (21-24).

#### *Fluorescence spectroscopy*

Measurements were performed with an FP-6200 spectrofluorimeter (Jasco, Japan) in a Peltier-thermostated cell holder, using a Quartz SUPRASIL 105.251-QS (Hellma) as described elsewhere (56). A bandwidth of 5 nm was used for the excitation and emission beams. For tryptophan intrinsic fluorescence and tryptophan fluorescence quenching by KI, the excitation wavelength was fixed at 290 nm. The emission spectra were recorded at 25 °C, from 300 to 400 nm at a scan rate of 125 nm.min<sup>-1</sup>. For ANS fluorescence (5 μM ANS; 0.5 μM CyaA), the excitation wavelength was fixed at 360 nm. The emission spectra were recorded from 450 to 550 nm.

The renaturation of CyaA was initiated by directly diluting the CyaA protein (10 μM stored in 8 M urea, 20 mM Hepes, pH 7.4) to a final concentration of 0.5 μM into either buffer A (20 mM Hepes, 150 mM NaCl, pH 7.4) or buffer B (buffer A plus 2 mM CaCl<sub>2</sub>) supplemented with the appropriate quantity of the chaotropic agent to obtain the final urea concentration. Samples were equilibrated for 2 hours at 25 °C before fluorescence measurements. The buffer A (or buffer B) supplemented with the targeted urea concentration was used as blank and its spectrum was subtracted to each protein fluorescence spectrum. The maximum emission wavelength ( $\lambda_{\max}$ ) values represent the average of three values obtained from emission spectra that were corrected for blank measurements.

#### *Synchrotron Radiation Circular Dichroism spectroscopy*

Synchrotron Radiation Circular dichroism (SR-CD) spectra were recorded on DISCO beamline at the synchrotron facility SOLEIL, (Gif-sur-Yvette, France). The SR-CD experiments were carried out at 25°C, integration time of 1200 msec and a bandwidth of 1 nm with a 1 nm resolution-step. Each far-UV spectrum represents the average of 3 scans of CyaA at 5 μM. Optical cell with a 26 μm path-length and CaF<sub>2</sub> windows (Hellma) were used for recording CD signals in far-UV region (from 180 to 260

nm). The CD units used were the mean residue ellipticity (MRE), expressed in kilodegrees square centimeter per decimole and per aminoacids ((Kdeg\*cm<sup>2</sup>)/(dmol\*aa)) and calculated as previously described (57). The far-UV CD spectrum was deconvoluted using K2D3 (58) and secondary structure predictions were performed with SOPMA (59).

#### *Circular dichroism spectroscopy*

CD spectra were recorded on an Aviv circular dichroism spectrometer model 215, equipped with a water-cooled Peltier unit as described elsewhere (17). CD measurements were carried out at a scan rate of 0.5 nm/sec (step: 0.5 nm and integration time: 1 sec) with a time constant of 100 msec and a bandwidth of 1 nm. Each far-UV and near-UV CD spectrum represents the average of at least 5 scans. Far-UV and near-UV CD spectra (CyaA: 1 μM) were recorded in rectangular quartz Suprasil cells of 0.1 mm and 1 cm path lengths (106.QS and 114B.QS, Hellma). To follow the renaturation of CyaA, the stock solution (10 μM in 8 M urea, 20 mM Hepes, pH 7.4) was directly diluted to a final concentration of 1 μM either in buffer A or in buffer B adjusted with the appropriate concentration of urea. CD spectra were recorded after 1 hour of equilibration at 25 °C. The buffer A or buffer B supplemented with the final urea concentrations were used as blank and their spectra were subtracted to each protein CD spectrum.

#### *Analytical ultracentrifugation*

Sedimentation velocity experiments were performed on a Beckman XL-A analytical ultracentrifuge (Beckman Coulter) in an AN60-Ti rotor at 25 °C. The samples were filtrated on 0.2 μm filters before experiments. Detection of the protein concentration as a function of radial position and time was performed by optical density measurements at a wavelength of 280 nm. The buffer was buffer A or buffer B. The computed viscosity and density of this buffer were (SEDNTERP 1.09) 0.908 cP and 1.004 g.mL<sup>-1</sup> at 25°C, respectively. The CyaA stock solution (10 μM in 8 M urea, 20 mM Hepes, pH 7.4) was loaded onto a G25 column equilibrated in buffer A to remove urea and the collected CyaA samples (diluted to 400 μL at 1.4 μM) were supplemented or not with 2 mM CaCl<sub>2</sub>, loaded in a 1.2 mm-thick two channels epoxy

centerpiece and spun at 20,000 rpm. Data were analyzed with the Sedfit software using a continuous size distribution  $c(s)$  model (17). We used the Svedberg equation to estimate the molecular mass of the species identified by sedimentation velocity assuming a frictional ratio ranging from 1.2 to 3 as acceptable values (60).

*Size exclusion chromatography coupled on-line to a tetra detector array.*

Size exclusion chromatography (SEC) was carried out on TSK 4000SWxl (TOSOH, rigid spherical silica; particle size: 8  $\mu\text{m}$ ), Superdex200 10/300 and 5/150 (GE Healthcare Life Sciences, cross-linked agarose and dextran; particle size: 9-13  $\mu\text{m}$ ), Superose 6HR (GE Healthcare Life Sciences, agarose; particle size: 11-15  $\mu\text{m}$ ) and sephacryl S200 (GE Healthcare Life Sciences, copolymer of allyl dextran and N,N-methylenebisacrylamide; particle size: 25-75  $\mu\text{m}$ ) media. SEC was controlled by a GPCmax module connected on-line to a tetra detector array (TDA) model 302 (Malvern Instruments Ltd). The oven of the TDA contained (i) a static light scattering cell with two photodiode detectors, at 7° for low angle (LALS) and at 90° for right angle laser light scattering (RALS), (ii) a deflection refractometer, (iii) a photometer and (iv) a differential viscometer. Protein concentration was determined using both the photometer and the deflection refractometer. The RALS data coupled to the concentration provided the molecular mass. The SEC is also coupled on-line to a QELS detector ( $\mu\text{V}$ , Malvern Instruments Ltd), which provided the hydrodynamic radius. CyaA samples in 8 M urea or after dialysis, dilution or desalting were analyzed by SEC-TDA, following the procedures described elsewhere (25,60,61). Briefly, all solutions were filtered on 0.2  $\mu\text{m}$  filters and allowed to equilibrate at 20 °C before SEC experiments and sample analyses were performed at 25°C in the oven of the TDA. All experimental sequences comprised calibration injections of BSA and PEO used for TDA calibration (200  $\mu\text{L}$  at 2 mg/mL). All data were acquired and processed using the Omnisec software (Malvern Instruments Ltd).

The protein batches were prepared as followed. The dialyzed CyaA in buffer A or B was obtained by incubating an aliquot of CyaA in 8M urea, 20 mM Hepes, pH 7.4 in Float-A-Lyzer G2. The desalted CyaA in buffer A or B was prepared using a 5 mL bed volume G25SF column.

*Hemolysis and intoxication assays*

The hemolytic and cytotoxic (i.e. ability to raise cAMP inside target cells) activities of the toxin were determined on sheep erythrocytes as described previously (8). Sheep erythrocytes were washed several times with buffer B and resuspended in this buffer at  $5 \times 10^8$  cells/ml. The different CyaA samples (i.e., CyaA renatured by G25 buffer exchange, oligomeric and monomeric CyaA species collected after refolding on TSK column) were directly diluted into the erythrocytes suspension to reach the final concentration (ranging from 0.03 to 30  $\mu\text{g/ml}$  for hemolytic activity and from 1 to 1000 ng/ml for the invasive activity). Control experiments were performed in the presence of excess EDTA (4 mM). The hemolytic activity was measured after an overnight incubation at 37 °C by quantifying the amount of hemoglobin released at 540 nm (and of intracellular content release at 405 nm). Complete lysis was obtained by addition of 0.1 % Triton X100.

The invasive activity was determined by measuring the intracellular cAMP accumulation. The erythrocytes suspensions were incubated with CyaA at 37 °C for 20 min, then cells were chilled on ice, centrifuged at 4°C at 2 500 rpm for 5 min, and resuspended in buffer A supplemented with 4 mM EDTA. The cells were centrifuged similarly and the pellets were resuspended in 200  $\mu\text{l}$  of buffer A plus 4 mM EDTA. After transfer into clean tubes, the samples were lysed with 400  $\mu\text{l}$  of 0.1 N HCl, and boiled for 5 min at 100 °C (to inactivate any remaining adenylate cyclase). The solutions were then neutralized by addition of 400  $\mu\text{l}$  of 0.1 N NaOH, and the insoluble material was removed by centrifugation at 14 000 rpm for 10 min. The intracellular cAMP content was determined by a competitive immunoassay using the “HitHunter® cAMP XS+ assay” kit (DISCOVER<sub>X</sub>) following the manufacturer instructions.

## Results

**1 - folding of CyaA by dilution, dialysis or desalting.** We first characterized the folding process of the CyaA toxin starting from the unfolded state in 8 M urea at neutral pH. The recombinant CyaA toxin used hereafter was produced in *E. coli* and purified essentially as previously described (see experimental procedures); an additional step of size-exclusion chromatography (SEC) in the presence of 8 M urea was added to improve the protein purity (see experimental procedures). The CyaA toxin was stored at  $-20^{\circ}\text{C}$  in 20 mM Hepes, 8 M urea, pH 7-8. We first investigated the refolding process of CyaA as a function of urea concentration in the absence (apo-state) and in the presence (holo-state) of calcium by intrinsic fluorescence of tryptophan, by ANS fluorescence and by far-UV circular dichroism (Figure 2). CyaA contains 15 tryptophan residues that can be used as a macroscopic probe of protein folding, while ANS fluorescence is sensitive to the presence of solvent-exposed apolar surfaces made of organized hydrophobic residues on the protein. The folding process was studied in 20 mM Hepes, 150 mM NaCl, pH 7.4 in the absence (buffer A) or in the presence of 2 mM  $\text{CaCl}_2$  (buffer B).

Both tryptophan and ANS fluorescence data showed that CyaA was unfolded in the presence of urea at concentrations higher than 4 M (Figure 2A and 2B) with an intrinsic fluorescence maximum emission wavelength at 355 nm typical of tryptophan side-chains fully exposed to the solvent and a maximum emission wavelength of ANS at 520 nm indicating the absence of solvent-exposed hydrophobic surface. Below 4 M urea, both tryptophan and ANS maximum emission wavelength of fluorescence changed, indicating that tryptophan residues were less exposed to the solvent, reaching a more apolar environment (Figure 2A) and that solvent-exposed hydrophobic patches were formed (Figure 2B). The main refolding steps of CyaA in the presence of calcium were initiated at 4 M and essentially completed at 2 M urea while in the absence of calcium the refolding appeared less cooperative, occurring between 4 and 0 M urea.

The refolding of CyaA was then explored by circular dichroism in the far-UV region. The CD spectra of CyaA in 6 M urea both with and without calcium were typical of unfolded proteins (Figure 2C). The far-UV CD spectra of CyaA after extensive dialysis against buffer in the absence or in the presence of 2 mM calcium, showed that CyaA had acquired significant secondary structure elements. The presence of a split  $\pi$ - $\pi^*$  band (above and below 200 nm) and the higher intensity of the  $n$ - $\pi^*$  band around 220 nm of the CD spectrum of the protein in the presence of calcium suggest a higher content of helical structure as compared to CyaA in the absence of calcium. The secondary structure content of CyaA upon refolding by dilution of urea was then followed at 220 nm as a function of urea concentrations (Figure 2D). The secondary structure changes as a function of urea concentrations were similar to the tryptophan or ANS fluorescence changes, suggesting that the folding of secondary and tertiary structures occurred in a concerted manner.

We further analyzed the various CyaA batches by size exclusion chromatography (SEC) followed by a tetra detector array (TDA). The right angle static laser light scattering (RALS) combined with the UV detector signals allows molecular mass determination while the quasi-elastic light scattering (QELS) provides the hydrodynamic radius ( $R_H$ ) of the eluting species. CyaA (in 8 M urea) when loaded on a TSK column equilibrated in 20 mM Hepes, 150 mM NaCl, 4 M urea, pH 7.4 eluted as a broad peak with a molecular mass of  $180 \pm 10$  kDa (Figure 3A) and an averaged  $R_H$  of  $12 \pm 2$  nm (Figure 3B and Table 1), indicating that CyaA in these conditions was monomeric and unfolded. Noteworthy, this  $R_H$  value of urea-unfolded CyaA corresponds to the expected value for an urea-unfolded protein of that size ((62) and see Table 1). CyaA was then dialyzed against buffer A or B (i.e., in the absence or in the presence of 2 mM calcium) and analyzed similarly by SEC-TDA. The CyaA dialyzed without calcium eluted mainly as multimeric species with molecular masses ranging between 500 and 2000 kDa (Figure 3C). A similar profile was observed with the CyaA dialyzed in the presence of calcium, albeit a weak peak around 14 mL likely

corresponding to a monomeric form could be detected (Figure 3D).

In an other set of experiments, the urea was removed from the CyaA samples by using a rapid buffer exchange by chromatography on a Sephadex G-25 Superfine desalting column instead of the dialysis procedure. The desalted CyaA samples were then analyzed similarly by SEC-TDA on the TSK column. As shown in Figure 3E & 3F, CyaA refolded by buffer exchange in the absence of calcium eluted mainly as multimers while a significant quantity of monomeric forms could be detected in the sample desalted in the presence of calcium. Collectively, these data indicate that although the urea-unfolded state was monomeric, upon removal of urea by dialysis or by a desalting procedure, CyaA formed mainly multimeric species both in calcium-free or in calcium-containing buffers, in agreement with prior studies (37,48).

Analytical ultracentrifugation (AUC) was performed to further analyze the CyaA samples obtained by refolding through the gel filtration buffer exchange procedure (Figures 3E and 3F). AUC was done either in the absence (Figure 4A and 4B) or in the presence of 2 mM calcium (Figure 4C and 4D). The distribution of sedimentation coefficients (Figure 4E) shows that in the absence of calcium, the main population is centered on 12 S corresponding to multimers, mainly dimers to tetramers while a weak population around 6 S, may correspond to a monomeric species in the apo-state. In the presence of calcium, a broad distribution of multimers was observed from 10 to 45 S with a minor peak at 7-8 S possibly corresponding to the monomeric population of holo-CyaA (see experimental procedures).

**2- Molecular confinement is required to produce monomeric CyaA.** The results described above showed that CyaA folding is initiated below 4 M urea with a concomitant formation of secondary and tertiary structures, and appearance of solvent-exposed hydrophobic surfaces that are probably involved in the aggregation process leading to the multimeric states of CyaA. We hypothesized that molecular confinement of CyaA during the refolding

process could decrease the intermolecular interactions between the polypeptides and could thus reduce potential aggregation. An experimental approach to confine proteins is to use gel filtration on matrix characterized by small particle and pore sizes. To test this hypothesis, we directly loaded the unfolded CyaA (in 8 M urea) onto a TSK 4000SWxl column made of a matrix of particle size of 8  $\mu\text{m}$  and pore size dimension of  $\approx 45$  nm (see experimental procedures) and equilibrated in buffer B. Figure 5A shows the UV and molecular mass profiles of CyaA chromatographed on the TSK column. In these conditions we observed multimeric forms eluting from 9 to 13 mL and a significant fraction of a monomeric species eluting between 13 and 15 mL ( $M$ :  $180 \pm 20$  kDa). The hydrodynamic radius of the monomeric CyaA species measured by dynamic light scattering was  $5.2 \pm 0.3$  nm (Table 1). This  $R_H$  value is slightly higher than expected for a folded and globular native protein of 1706 residues ((62) and see Table 1). This excess of friction might be related to CyaA shape and/or hydration (see (61) for details and legend of Table 1). We further showed that the monomeric holo-CyaA toxin was stable for long-term storage at  $-20^\circ\text{C}$  as its hydrodynamic radius and its retention volume by SEC were identical before and after thawing.

We further analyzed the impact of the initial concentration of CyaA on the multimer/monomer ratio. Samples of CyaA at concentrations of 12, 5, 2.5 or 1  $\mu\text{M}$  in 8 M urea were loaded on the TSK column equilibrated in buffer B. Figure 5C shows that the proportion of monomers versus multimers was dependent upon the initial concentration of the urea-unfolded CyaA loaded onto the column. The four SEC profiles of CyaA show that the fraction of multimers increased with the initial CyaA concentration, suggesting that the multimer formation is an aggregative process.

Figure 6A compares the UV-profiles on SEC-TDA obtained by the three methods used to refold CyaA, i.e., by dialysis, by buffer exchange onto G-25 or by direct loading onto the TSK column. It is noteworthy that the proportion of monomers appears to be related to the molecular confinement during refolding as a higher fraction

of monomeric CyaA was obtained with the TSK matrix with smaller particle size (8  $\mu\text{m}$ ) as compared to G-25 matrix (52  $\mu\text{m}$ ) or to the absence of confinement in the case of dialysis procedure. The TSK column is made of rigid spherical silica beads bonded with hydrophilic groups, while the Sephadex G-25 is a bead-formed gel made of epichlorohydrin cross-linked dextran. To determine whether the chemical nature of the matrix may also contribute to the formation of monomeric CyaA in addition to the confinement effect, we compared results obtained on the TSK column with those obtained on a Superdex200 resin, made of cross-linked dextran and agarose with particle size of 11  $\mu\text{m}$ . As shown in Figure 6B, the urea-denatured CyaA loaded and refolded onto the Superdex200 10/300 column eluted as both multimers (8-11 mL) and monomer (12 mL) as observed with the TSK column. To further test the confinement-dependent refolding, CyaA was analyzed by SEC on Superdex200 after protein dialysis in the presence of calcium. The Superdex200 chromatogram clearly shows that dialysis of CyaA produced only multimers (Figure 6B). These results indicate that the confinement properties of the matrix (TSK or Superdex200) rather than its chemical nature are important for efficient folding of CyaA into a monomeric form.

The confinement effect was further evaluated by comparing the CyaA folding process on Superdex200 and on a Sephacryl200 column, the latter having a similar chemical nature (agarose and dextran) and similar optimum protein separation range as the Superdex resin but with larger particle size ( $50 \pm 25 \mu\text{m}$  for Sephacryl vs 11  $\mu\text{m}$  for Superdex). The UV profiles obtained with the Sephacryl200 and the Superdex200 (packed in the same XK16/60 column to strictly compare the experiments) are superimposed in Figure 6C and clearly demonstrate that the confinement provided by the Superdex matrix by reducing intermolecular interactions strongly favored monomer formation as compared to the Sephacryl medium, which only produced multimers. Refolding of CyaA on a Superose 6HR column made of agarose beads with particle size of  $13 \pm 2 \mu\text{m}$  (similar to

Superdex200) also favored the folding of the protein into a monomeric state (Figure 6D). Taken together, these data indicate that molecular confinement during CyaA refolding on SEC may reduce intermolecular interactions between proteins and thus favor folding of the toxin into a monomeric state. The confinement properties appear rather independent of the chemical composition of the matrix (silica, agarose, dextran).

### ***3- Calcium and acylation are required for CyaA folding into a monomeric form.***

Besides molecular confinement, we investigated the parameters that could affect the efficiency of formation of CyaA monomers. CyaA is known to require calcium and acylation for its toxic activities, i.e. cell lysis (hemolysis) and delivery of its catalytic domain across the plasma membrane into the cytosol to produce cAMP (intoxication). The effect of calcium on CyaA folding is illustrated by the SEC profiles of CyaA refolded on Superdex200 5/150 column equilibrated in the absence or in the presence of 2 mM calcium (Figure 7A). The comparison of the SEC profiles shows that the presence of calcium was crucial for CyaA refolding. The refolding properties of pro-CyaA, i.e., the toxin without acyl chains, were then investigated (Figure 7B). The post-translational acylation of pro-CyaA, leading to the mature CyaA protein, is well known to be essential for toxin activity. However, its impact on the folding of CyaA has never been investigated. We first measured the molecular mass of pro-CyaA in 4 M urea. The SEC-TDA data showed that pro-CyaA was monomeric in 4 M urea (not shown), as observed for the acylated CyaA (Figure 3A). The SEC profile of pro-CyaA upon refolding onto Superdex200 in the presence of 2 mM calcium shows two species (Figure 7B, thick trace), the main peak corresponding to large multimers and the second peak, appearing as a shoulder on the main peak of multimers, corresponds to species of smaller sizes. However, in marked contrast to the acylated CyaA (Figure 7A, thick trace), no distinct peak corresponding to a monomeric pro-CyaA species could be evidenced. Finally, refolding of CyaA and pro-CyaA in the absence of calcium was also examined and showed that

both proteins refolded in EDTA led to the formation of multimers (Figure 7A and 7B, dashed traces). Collectively, these data indicate that besides molecular confinement, both acylation and calcium are required to produce high yields of CyaA monomers.

#### ***4- Structural and functional characterization of the monomeric state of CyaA.***

We then analyzed by synchrotron radiation circular dichroism the secondary structure content of the monomeric CyaA species isolated from the SEC-assisted folding procedure (monomeric fraction M, eluting at 12-13 ml on the Superdex200 chromatography shown in Figure 6C). The far-UV CD spectrum of CyaA is typical of an alpha/beta protein (Figure 8), as suggested by the CD spectrum deconvolution performed by K2D3. The secondary structure content estimation obtained from the deconvolution is close to the secondary structure content of CyaA predicted by SOPMA (see legend of Figure 8). We also analyzed the far-UV CD spectrum of the multimeric CyaA species (oligomeric fraction O, eluting at 7-9 ml in Figure 6C). Both monomers and multimers exhibit similar far-UV CD spectra (inset Figure 8) indicating that the secondary structure content of CyaA is not significantly affected by the oligomerisation state (quaternary structure) of the molecule.

The tertiary structure contents of CyaA in the urea-unfolded, monomeric or multimeric states were then analyzed by near-UV CD (Figure 8B). The near-UV CD spectrum of the urea-unfolded CyaA shows weak dichroic phenylalanine <sup>1</sup>Lb bands at 262 and 268 nm and tryptophan <sup>1</sup>Lb bands around 285 and 292 nm. Such weak intensities are expected for a urea-unfolded protein, indicating a low content of tertiary structure. The near-UV CD spectra of the folded monomeric and multimeric CyaA toxins exhibit similar strong dichroic bands, although the monomeric state provides more intense dichroic bands. The near-UV CD spectra show broad tyrosine <sup>1</sup>Lb bands centered at 280 nm and tryptophan <sup>1</sup>Lb bands around 285 and 292 nm (shifted to 295 nm due to the slope of the tyrosine <sup>1</sup>Lb band). These near-UV CD data indicate that once CyaA is refolded, several

aromatic side-chains are involved in tertiary structure constraints. These results also indicate that the monomeric and oligomeric states of CyaA cannot be distinguished from their CD spectra neither in the far nor in the near-UV region.

We also probed the accessibility of tryptophans by fluorescence quenching using KI as quencher. As shown in figure 8C and 8D, the tryptophan side chains are more accessible to KI quenching in the monomeric CyaA than in the oligomeric ones. This suggests that as a result of multimerization, some tryptophans of CyaA became buried in oligomers and thus less accessible to collisional quenching than in the monomeric state.

Finally, the biological activities of the different CyaA species were compared using sheep erythrocytes as model target cells. The oligomeric (O) and monomeric (M) CyaA fractions, eluted from the Superdex200 column (Figure 6C), were independently pooled, concentrated and assayed for activity. For each species, both the hemolytic activity (i.e. ability to lyse cells) and the capacity of the toxin to increase intracellular cAMP (invasive activity) were monitored as a function of protein concentrations. CyaA refolded by rapid buffer exchange on G25 in the absence or in the presence of calcium was also tested in parallel. Figure 9 shows that the refolded monomeric CyaA (fraction M) displayed the highest hemolytic and cytotoxic activities: its specific hemolytic and cytotoxic activities were about 20-25 times higher than that of the multimeric fractions (fraction O). CyaA refolded by rapid buffer exchange on G25 in the presence of calcium exhibited similar hemolytic activity as the oligomers from SEC and was rather inefficient to induce cAMP production (Figure 9, triangles). CyaA refolded by rapid buffer exchange on G25 in the absence of calcium exhibited neither hemolytic nor cytotoxic activities, in agreement with previous data showing that calcium is required for both activities.

It should be noted that the hemolytic activity shows a cooperativity ( $n \sim 3$ ) in agreement with prior reports suggesting that pore formation requires oligomerisation of the protein

in the membrane. In contrast the accumulation of intracellular cAMP did not display any cooperativity, in line with the idea that the competent form able to translocate its catalytic domain across the plasma membrane is the monomeric state of CyaA. All together these data indicate that the refolded, monomeric state of CyaA exhibits the highest hemolytic and cell-invasive activities and might be therefore considered as the genuine, functionally active form of the toxin.

**Discussion.** We report here a procedure to produce a monomeric form of *B. pertussis* CyaA toxin that exhibits high hemolytic and cytotoxic activities and that can be stably maintained in this functional monodisperse state in the absence of any chaotropic agent. Since the original description of the adenylate cyclase in *B. pertussis* in the early eighties, numerous reports have highlighted the heterogeneity of the molecular forms of this toxin that appeared to be prone to aggregation into multimeric non-functional complexes (37,48,52). Indeed, CyaA is a large protein of 1706 amino-acid residues that contains several markedly hydrophobic regions as well as two post-translationally added acyl groups. Due to these characteristics, CyaA has been mostly extracted, purified and stored in the presence of high concentration of chaotropic agent (usually urea) to prevent its aggregation. In initial works, CyaA was purified from urea extracts from wild-type *B. pertussis* bacteria (6,48,51,52). Later, after cloning of the *cyaA* gene in the late eighties, CyaA has been largely produced as a recombinant protein in *E. coli*, also co-expressing CyaC to permit its post-translational acylation (53,63). In these recombinant cells, CyaA mainly accumulates as inclusion bodies requiring denaturing conditions for its solubilization. In most of these studies, the protein batches were stored after purification in buffers containing urea (higher than 6 M) to maintain it in a soluble form. The cytotoxic activities of CyaA have been usually tested by directly diluting the stock solution of toxin into cell suspensions without taking special care about its refolding process and/or its final oligomeric status. Even biological assays of CyaA toxin or CyaA-based vaccines (64-66) in

animals have been carried out with recombinant CyaA preparations that were extemporaneously diluted in physiological buffers just before administration. How the toxin refolds and what are the precise molecular forms achieved by CyaA in these conditions remained largely unexplored.

Here we have characterized the refolding process of CyaA with the hope to identify conditions that might favor its folding as a monomeric form suitable for further structural, biochemical and cellular characterization. Our results showed that CyaA is unfolded and monomeric in urea concentration higher than 4 M (Figure 3 and Table 1), with a hydrodynamic radius of  $12 \pm 2$  nm, in good agreement with the expected hydrodynamic radius for a protein of 177 kDa unfolded in urea (62) (25,67). The folding of CyaA in the presence of calcium, as revealed by the acquisition of secondary structure elements and the formation of solvent-exposed hydrophobic patches, occurs at urea concentrations lower than 4 M and is essentially completed at 2 M (Figure 2). Characterization of the hydrodynamic properties of the protein refolded upon urea removal either through dialysis, dilution or rapid buffer exchange on desalting column, indicated that in all these conditions CyaA mainly formed multimers, from tetramers to higher order oligomers, as reported earlier (37,48).

With the aim of decreasing CyaA intermolecular interactions during urea removal and thus reducing the aggregative processes, we explored an alternative approach that involved molecular confinement of the protein during its refolding process. We found that refolding of urea-unfolded CyaA by size-exclusion chromatography on resins with small particle and pore sizes (beads of different chemical nature with diameters from 8 to 15  $\mu$ m on average) resulted in a significant fraction of the molecules eluting as a monomeric species with an apparent hydrodynamic radius of  $5.2 \pm 0.3$  nm, as determined by dynamic light scattering. Interestingly, the fraction of monomeric species thus obtained appeared to be inversely correlated with the protein concentration of the sample loaded on the SEC column, suggesting that the formation of CyaA multimers is likely an

aggregative process. This aggregation propensity is probably due to the appearance of solvent-exposed hydrophobic surfaces during the refolding process as indicated by the ANS studies. More importantly, the folding of CyaA into a monomeric form was found to be critically dependent upon the presence of calcium as well as on the post-translational acylation of the protein. We further showed that, although the secondary structure content of the monomeric and multimeric species is rather similar, the monomeric form displayed about 20-25 times higher hemolytic and cytotoxic activities than the multimeric ones. This suggests that the refolded CyaA monomer is the genuine, physiologically active form of the toxin.

Interestingly, the hemolytic activity shows a marked cooperativity ( $n_H \sim 3$ ) as a function of CyaA monomer concentration, indicating that, in accordance with prior studies, the membrane permeabilizing capacity requires oligomerisation of the toxin. The fact that the monomeric state, in solution, of CyaA exhibits a much higher lytic potency than the multimeric ones, suggests that the oligomerization of the protein might take place within the lipid bilayer, once monomers have partitioned into membranes. The conformations of membrane-inserted oligomers of CyaA are likely distinct from CyaA multimers formed in solution as the latter are less hemolytic. Previously, Sebo and colleagues (40) proposed that the lytic activity of CyaA may be carried out by a dedicated oligomeric conformation of CyaA, pre-existing in solution, while the invasive activity would be mainly displayed by a distinct monomeric conformation. At variance, our present observations suggest that the monomeric state in solution, rather than the oligomeric state, is endowed with both the lytic and cytotoxic activities of CyaA. CyaA oligomerization within the membrane might then lead to the pore-forming state whereas the monomeric CyaA is likely the competent form able to translocate its catalytic domain across the plasma membrane of the target cells, as suggested by the lack of cooperativity of intracellular cAMP accumulation.

We thus propose the following model. The CyaA monomer in solution is the functional state that partitions into the membrane mainly via

hydrophobic forces, involving its hydrophobic regions. Once CyaA is membrane-inserted, the translocation region may locally destabilize the lipid bilayer favoring the passage of the catalytic domain across the plasma membrane (8,9). Meanwhile, CyaA monomers can interact and reorganize into oligomers within the membrane. These CyaA oligomers may lead to pore formation that ultimately induces cell lysis (1). This sequential model fits nicely with the observed delay between the kinetics of cAMP accumulation and of hemolysis (6). Yet, further works will be needed to characterize the oligomerization process of CyaA within the membrane and its relation to functions.

Our present data provide a rationale explanation for many prior observations on CyaA structure-function relationships and may also have important implications for the understanding of the role of calcium and acylation in the biological functions of other RTX cytolysins (14). Indeed, it has been known for many years that RTX cytolysins such as CyaA, HlyA, LktA, etc..., are synthesized as inactive precursors that are converted to their cytotoxic forms upon acylation by dedicated acyltransferase, (CyaC, HlyC, LktC, etc...) and that their cytotoxic/cytolytic activities are critically dependent upon the presence of calcium (14,15). We and others previously showed that calcium is essential for folding of the CyaA RTX-domain, RD, which is important for protein interaction with the CyaA receptor and/or with target cell membrane. Our present work indicates that calcium binding to the RD domain directly contributes to the overall folding of the full-length toxin into a monomeric, active species. It is likely that in the presence of calcium, RD can acquire its calcium-bound 3D structure that can then serve as a nucleation site for further folding of the upstream CyaA regions, i.e. the central hydrophobic and N-terminal catalytic domains. Incidentally, this proposed sequential refolding scheme fits with the idea that CyaA, like other RTX proteins, is secreted by the type I secretion machinery (T1SS) in a vectorial C- to N-terminal way, with its C-terminus reaching first the external, calcium-rich environment. Calcium-dependent folding of the secreted RD domain likely begins

as it emerges from the secretion channel and while the remaining CyaA polypeptide is still in transit in the T1SS machinery. The folded RD may thus drive the progressive folding of the upstream CyaA regions as they exit the secretory channel. This co-secretional folding of CyaA at the mouth of the T1SS machinery could contribute to the confinement of the toxin molecules and thus prevent their potential aggregation at the bacterial surface. Interestingly, Gray et al. showed that only the toxin that is actively secreted by *B. pertussis* by the T1SS pathway is able to invade eukaryotic cells (68). It is tempting to speculate that this invasive, actively secreted species described by these authors indeed correspond to the monomeric CyaA toxin.

Besides calcium and molecular confinement, a major finding reported here is that CyaA acylation appears to be critical for toxin folding into the monomeric form. Indeed, we were not able to produce proCyaA monomers or to isolate them from multimers, as we did with the acylated CyaA. These results thus establish for the first time, a direct structural role for the acyl chains in the acquisition of a biologically functional conformation by CyaA, independently of, or in addition to, their putative role(s) in membrane interaction. This result is in line with the seminal observation of Rogel et al. (37) who first reported the purification of the toxic form of adenylate cyclase from *B. pertussis* extracts. By gel filtration, they resolved the enzymatic activity into two peaks, one major peak of high molecular weight (> 700kDa) and a minor peak, with an apparent size of 200 kDa. They showed that, although both fractions contained the same CyaA polypeptide, only the small-size fraction could induce cAMP accumulation in target cells (37). As the CyaA polypeptide expressed in *E. coli* also lack the ability to induce cAMP accumulation in target cells, they postulated that a post-translational modification should occur in *B. pertussis* but not in *E. coli*, to confer cytotoxic capabilities to CyaA. The CyaC modifying acyltransferase and the specific acylation of CyaA on lysine residues 860 and 983 were later described by E. Hewlett and colleagues (10). How this modification could convert the non-cytotoxic pro-CyaA into

an invasive and hemolytic protein has remained elusive until now (14,15). Similar observations have been reported for other RTX cytolysins, in particular for HlyA, but the putative contribution of the acyl chains in the cytolytic activities of these toxins is also still unknown. It is generally assumed that the acyl chains could insert into the lipid bilayer to favor toxin partitioning to the plasma membrane of target cells (69). Alternatively, the acyl groups might play a structural role in maintaining the toxins in a partially folded conformation competent for membrane insertion (14,15). No strong experimental evidence for this hypothesis has been obtained thus far. Herlax and Bakas tentatively proposed that the acylation may maintain HlyA in a molten globule conformation favorable for membrane insertion, but their experimental data barely support such a conclusion (70).

Our present work suggests possible molecular mechanisms by which the acyl chains and calcium binding may accelerate the kinetics of CyaA refolding and thus favor the overall formation of functional monomeric species at the expense of the less-active multimeric ones. The presence of hydrophobic acyl chains on CyaA may significantly modify the local free-energy landscape of the polypeptide chain. Shielding of these acyl chains into a nascent hydrophobic core may have a major thermodynamic contribution in restricting the temporal and conformational spaces accessible to CyaA upon refolding. Similarly, we provide direct evidence that calcium binding is mandatory for the formation of monomers, probably by kinetically favoring native folding and burying of hydrophobic regions, while in the absence of calcium, a slower kinetics of folding into the apo-state may favor intermolecular interactions between folding intermediates and would thus increase the population of multimer species. Further studies will be needed to unravel the respective contributions of calcium and acylation to the CyaA folding pathways.

Finally, the ability to produce CyaA as a functional and monodisperse species that appears to be sufficiently stable for in-depth biophysical, structural and cellular characterizations will be invaluable to clarify the

fundamental basis of its mode of action. Besides, our current results will also be instrumental for further biotechnological improvements of CyaA

as a vaccine vehicle for antigen delivery to dendritic cells, a novel vaccine strategy that is currently evaluated in clinical trials.

### Acknowledgements

We acknowledge SOLEIL for provision of synchrotron radiation facilities (Proposal ID 20110586 and 20120444) and we thank Frank Wien for assistance in using Disco beamline. We thank Agnes Ullmann for critical reading of the manuscript. The project was supported by the Agence Nationale de la Recherche, programme Jeunes Chercheurs (grant ANR-09-JCJC-0012), the Institut Pasteur Projet Transversal de Recherche PTR#374, Jacob class of Pasteur-Paris University International Ph.D. Program from Institut Pasteur, the Centre National de la Recherche Scientifique (CNRS UMR 3528, Biologie Structurale et Agents Infectieux).

### References

1. Ladant, D., and Ullmann, A. (1999) Bordetella pertussis adenylate cyclase: a toxin with multiple talents. *Trends in microbiology* **7**, 172-176
2. Vojtova, J., Kamanova, J., and Sebo, P. (2006) Bordetella adenylate cyclase toxin: a swift saboteur of host defense. *Curr Opin Microbiol* **9**, 69-75
3. Carbonetti, N. H. (2010) Pertussis toxin and adenylate cyclase toxin: key virulence factors of Bordetella pertussis and cell biology tools. *Future Microbiol* **5**, 455-469
4. Glaser, P., Ladant, D., Sezer, O., Pichot, F., Ullmann, A., and Danchin, A. (1988) The calmodulin-sensitive adenylate cyclase of Bordetella pertussis: cloning and expression in Escherichia coli. *Molecular microbiology* **2**, 19-30
5. Glaser, P., Sakamoto, H., Bellalou, J., Ullmann, A., and Danchin, A. (1988) Secretion of cyclolysin, the calmodulin-sensitive adenylate cyclase-haemolysin bifunctional protein of Bordetella pertussis. *Embo J* **7**, 3997-4004
6. Bellalou, J., Sakamoto, H., Ladant, D., Geoffroy, C., and Ullmann, A. (1990) Deletions affecting hemolytic and toxin activities of Bordetella pertussis adenylate cyclase. *Infection and immunity* **58**, 3242-3247
7. Sakamoto, H., Bellalou, J., Sebo, P., and Ladant, D. (1992) Bordetella pertussis adenylate cyclase toxin. Structural and functional independence of the catalytic and hemolytic activities. *J Biol Chem* **267**, 13598-13602
8. Karst, J. C., Barker, R., Devi, U., Swann, M. J., Davi, M., Roser, S. J., Ladant, D., and Chenal, A. (2012) Identification of a region that assists membrane insertion and translocation of the catalytic domain of Bordetella pertussis CyaA toxin. *J Biol Chem* **287**, 9200-9212
9. Subrini, O., Sotomayor-Perez, A. C., Hessel, A., Spiaczka-Karst, J., Selwa, E., Sapay, N., Veneziano, R., Pansieri, J., Chopineau, J., Ladant, D., and Chenal, A. (2013) Characterization of a membrane-active peptide from the Bordetella pertussis CyaA toxin. *J Biol Chem* **288**, 32585-32598
10. Barry, E. M., Weiss, A. A., Ehrmann, I. E., Gray, M. C., Hewlett, E. L., and Goodwin, M. S. (1991) Bordetella pertussis adenylate cyclase toxin and hemolytic activities require a second gene, cyaC, for activation. *J Bacteriol* **173**, 720-726
11. Hackett, M., Guo, L., Shabanowitz, J., Hunt, D. F., and Hewlett, E. L. (1994) Internal lysine palmitoylation in adenylate cyclase toxin from Bordetella pertussis. *Science* **266**, 433-435

12. Masin, J., Basler, M., Knapp, O., El-Azami-El-Idrissi, M., Maier, E., Konopasek, I., Benz, R., Leclerc, C., and Sebo, P. (2005) Acylation of lysine 860 allows tight binding and cytotoxicity of Bordetella adenylate cyclase on CD11b-expressing cells. *Biochemistry* **44**, 12759-12766
13. Westrop, G. D., Hormozi, E. K., Da Costa, N. A., Parton, R., and Coote, J. G. (1996) Bordetella pertussis adenylate cyclase toxin: proCyaA and CyaC proteins synthesised separately in Escherichia coli produce active toxin in vitro. *Gene* **180**, 91-99
14. Welch, R. A. (2001) RTX toxin structure and function: a story of numerous anomalies and few analogies in toxin biology. *Current topics in microbiology and immunology* **257**, 85-111
15. Linhartova, I., Bumba, L., Masin, J., Basler, M., Osicka, R., Kamanova, J., Prochazkova, K., Adkins, I., Hejnova-Holubova, J., Sadilkova, L., Morova, J., and Sebo, P. (2010) RTX proteins: a highly diverse family secreted by a common mechanism. *FEMS Microbiol Rev* **34**, 1076-1112
16. Rose, T., Sebo, P., Bellalou, J., and Ladant, D. (1995) Interaction of calcium with Bordetella pertussis adenylate cyclase toxin. Characterization of multiple calcium-binding sites and calcium-induced conformational changes. *J Biol Chem* **270**, 26370-26376
17. Chenal, A., Guijarro, J. I., Raynal, B., Delepierre, M., and Ladant, D. (2009) RTX calcium binding motifs are intrinsically disordered in the absence of calcium: implication for protein secretion. *J Biol Chem* **284**, 1781-1789
18. Szilvay, G. R., Blenner, M. A., Shur, O., Cropek, D. M., and Banta, S. (2009) A FRET-based method for probing the conformational behavior of an intrinsically disordered repeat domain from Bordetella pertussis adenylate cyclase. *Biochemistry* **48**, 11273-11282
19. Chenal, A., Karst, J. C., Sotomayor Perez, A. C., Wozniak, A. K., Baron, B., England, P., and Ladant, D. (2010) Calcium-induced folding and stabilization of the intrinsically disordered RTX domain of the CyaA toxin. *Biophys J* **99**, 3744-3753
20. Sotomayor-Perez, A. C., Subrini, O., Hessel, A., Ladant, D., and Chenal, A. (2013) Molecular Crowding Stabilizes Both the Intrinsically Disordered Calcium-Free State and the Folded Calcium-Bound State of a Repeat in Toxin (RTX) Protein. *Journal of the American Chemical Society* **135**, 11929-11934
21. Linding, R., Russell, R. B., Neduva, V., and Gibson, T. J. (2003) GlobPlot: Exploring protein sequences for globularity and disorder. *Nucleic Acids Res* **31**, 3701-3708
22. Prilusky, J., Felder, C. E., Zeev-Ben-Mordehai, T., Rydberg, E. H., Man, O., Beckmann, J. S., Silman, I., and Sussman, J. L. (2005) FoldIndex: a simple tool to predict whether a given protein sequence is intrinsically unfolded. *Bioinformatics (Oxford, England)* **21**, 3435-3438
23. Dosztanyi, Z., Csizmok, V., Tompa, P., and Simon, I. (2005) The pairwise energy content estimated from amino acid composition discriminates between folded and intrinsically unstructured proteins. *Journal of molecular biology* **347**, 827-839
24. Lieutaud, P., Canard, B., and Longhi, S. (2008) MeDor: a metaserver for predicting protein disorder. *BMC Genomics* **9 Suppl 2**, S25
25. Sotomayor-Perez, A. C., Ladant, D., and Chenal, A. (2011) Calcium-induced folding of intrinsically disordered repeat-in-toxin (RTX) motifs via changes of protein charges and oligomerization states. *J Biol Chem* **286**, 16997-17004

26. Baumann, U., Wu, S., Flaherty, K. M., and McKay, D. B. (1993) Three-dimensional structure of the alkaline protease of *Pseudomonas aeruginosa*: a two-domain protein with a calcium binding parallel beta roll motif. *EMBO J* **12**, 3357-3364
27. Meier, R., Drepper, T., Svensson, V., Jaeger, K. E., and Baumann, U. (2007) A calcium-gated lid and a large beta-roll sandwich are revealed by the crystal structure of extracellular lipase from *Serratia marcescens*. *J Biol Chem* **282**, 31477-31483
28. Satchell, K. J. (2011) Structure and function of MARTX toxins and other large repetitive RTX proteins. *Annual review of microbiology* **65**, 71-90
29. Holland, I. B., Schmitt, L., and Young, J. (2005) Type 1 protein secretion in bacteria, the ABC-transporter dependent pathway (review). *Mol Membr Biol* **22**, 29-39
30. Masure, H. R., Au, D. C., Gross, M. K., Donovan, M. G., and Storm, D. R. (1990) Secretion of the *Bordetella pertussis* adenylate cyclase from *Escherichia coli* containing the hemolysin operon. *Biochemistry* **29**, 140-145
31. Guermonprez, P., Khelef, N., Blouin, E., Rieu, P., Ricciardi-Castagnoli, P., Guiso, N., Ladant, D., and Leclerc, C. (2001) The adenylate cyclase toxin of *Bordetella pertussis* binds to target cells via the alpha(M)beta(2) integrin (CD11b/CD18). *J Exp Med* **193**, 1035-1044
32. Rogel, A., and Hanski, E. (1992) Distinct steps in the penetration of adenylate cyclase toxin of *Bordetella pertussis* into sheep erythrocytes. Translocation of the toxin across the membrane. *J Biol Chem* **267**, 22599-22605
33. Basler, M., Knapp, O., Masin, J., Fiser, R., Maier, E., Benz, R., Sebo, P., and Osicka, R. (2007) Segments crucial for membrane translocation and pore-forming activity of *Bordetella* adenylate cyclase toxin. *J Biol Chem* **282**, 12419-12429
34. Eby, J. C., Ciesla, W. P., Hamman, W., Donato, G. M., Pickles, R. J., Hewlett, E. L., and Lencer, W. I. (2010) Selective translocation of the *Bordetella pertussis* adenylate cyclase toxin across the basolateral membranes of polarized epithelial cells. *J Biol Chem* **285**, 10662-10670
35. Paccani, S. R., Finetti, F., Davi, M., Patrussi, L., D'Elisio, M. M., Ladant, D., and Baldari, C. T. (2011) The *Bordetella pertussis* adenylate cyclase toxin binds to T cells via LFA-1 and induces its disengagement from the immune synapse. *J Exp Med* **208**, 1317-1330
36. Gordon, V. M., Young, W. W., Jr., Lechler, S. M., Gray, M. C., Leppla, S. H., and Hewlett, E. L. (1989) Adenylate cyclase toxins from *Bacillus anthracis* and *Bordetella pertussis*. Different processes for interaction with and entry into target cells. *J Biol Chem* **264**, 14792-14796
37. Rogel, A., Schultz, J. E., Brownlie, R. M., Coote, J. G., Parton, R., and Hanski, E. (1989) *Bordetella pertussis* adenylate cyclase: purification and characterization of the toxic form of the enzyme. *Embo J* **8**, 2755-2760
38. Guermonprez, P., Ladant, D., Karimova, G., Ullmann, A., and Leclerc, C. (1999) Direct delivery of the *Bordetella pertussis* adenylate cyclase toxin to the MHC class I antigen presentation pathway. *J Immunol* **162**, 1910-1916
39. Bauche, C., Chenal, A., Knapp, O., Bodenreider, C., Benz, R., Chaffotte, A., and Ladant, D. (2006) Structural and functional characterization of an essential RTX subdomain of *Bordetella pertussis* adenylate cyclase toxin. *J Biol Chem* **281**, 16914-16926
40. Vojtova-Vodolanova, J., Basler, M., Osicka, R., Knapp, O., Maier, E., Cerny, J., Benada, O., Benz, R., and Sebo, P. (2009) Oligomerization is involved in pore formation by *Bordetella* adenylate cyclase toxin. *Faseb J* **23**, 2831-2843

41. Bumba, L., Masin, J., Fiser, R., and Sebo, P. (2010) Bordetella adenylate cyclase toxin mobilizes its beta2 integrin receptor into lipid rafts to accomplish translocation across target cell membrane in two steps. *PLoS Pathog* **6**, e1000901
42. Veneziano, R., Rossi, C., Chenal, A., Devoisselle, J. M., Ladant, D., and Chopineau, J. (2013) Bordetella pertussis adenylate cyclase toxin translocation across a tethered lipid bilayer. *Proc Natl Acad Sci U S A* **110**, 20473-20478
43. Uribe, K. B., Etxebarria, A., Martin, C., and Ostolaza, H. (2013) Calpain-Mediated Processing of Adenylate Cyclase Toxin Generates a Cytosolic Soluble Catalytically Active N-Terminal Domain. *PLoS One* **8**, e67648
44. Heveker, N., and Ladant, D. (1997) Characterization of mutant Bordetella pertussis adenylate cyclase toxins with reduced affinity for calmodulin. Implications for the mechanism of toxin entry into target cells. *European journal of biochemistry / FEBS* **243**, 643-649
45. Benz, R., Maier, E., Ladant, D., Ullmann, A., and Sebo, P. (1994) Adenylate cyclase toxin (CyaA) of Bordetella pertussis. Evidence for the formation of small ion-permeable channels and comparison with HlyA of Escherichia coli. *J Biol Chem* **269**, 27231-27239
46. Hewlett, E. L., Donato, G. M., and Gray, M. C. (2006) Macrophage cytotoxicity produced by adenylate cyclase toxin from Bordetella pertussis: more than just making cyclic AMP! *Molecular microbiology* **59**, 447-459
47. Fiser, R., Masin, J., Basler, M., Krusek, J., Spulakova, V., Konopasek, I., and Sebo, P. (2007) Third activity of Bordetella adenylate cyclase (AC) toxin-hemolysin. Membrane translocation of AC domain polypeptide promotes calcium influx into CD11b+ monocytes independently of the catalytic and hemolytic activities. *J Biol Chem* **282**, 2808-2820
48. Gentile, F., Knipling, L. G., Sackett, D. L., and Wolff, J. (1990) Invasive adenylate cyclase of Bordetella pertussis. Physical, catalytic, and toxic properties. *J Biol Chem* **265**, 10686-10692
49. Hewlett, E. L., Gray, L., Allietta, M., Ehrmann, I., Gordon, V. M., and Gray, M. C. (1991) Adenylate cyclase toxin from Bordetella pertussis. Conformational change associated with toxin activity. *J Biol Chem* **266**, 17503-17508
50. Cheung, G. Y., Kelly, S. M., Jess, T. J., Prior, S., Price, N. C., Parton, R., and Coote, J. G. (2009) Functional and structural studies on different forms of the adenylate cyclase toxin of Bordetella pertussis. *Microbial pathogenesis* **46**, 36-42
51. Hewlett, E. L., Urban, M. A., Manclark, C. R., and Wolff, J. (1976) Extracytoplasmic adenylate cyclase of Bordetella pertussis. *Proc Natl Acad Sci U S A* **73**, 1926-1930
52. Hewlett, E. L., Gordon, V. M., McCaffery, J. D., Sutherland, W. M., and Gray, M. C. (1989) Adenylate cyclase toxin from Bordetella pertussis. Identification and purification of the holotoxin molecule. *J Biol Chem* **264**, 19379-19384
53. Karimova, G., Fayolle, C., Gmira, S., Ullmann, A., Leclerc, C., and Ladant, D. (1998) Charge-dependent translocation of Bordetella pertussis adenylate cyclase toxin into eukaryotic cells: implication for the in vivo delivery of CD8(+) T cell epitopes into antigen-presenting cells. *Proc Natl Acad Sci U S A* **95**, 12532-12537
54. Ladant, D., Brezin, C., Alonso, J. M., Crenon, I., and Guiso, N. (1986) Bordetella pertussis adenylate cyclase. Purification, characterization, and radioimmunoassay. *J Biol Chem* **261**, 16264-16269

55. Semisotnov, G. V., Rodionova, N. A., Razgulyaev, O. I., Uversky, V. N., Gripas, A. F., and Gilmanshin, R. I. (1991) Study of the "molten globule" intermediate state in protein folding by a hydrophobic fluorescent probe. *Biopolymers* **31**, 119-128
56. Sotomayor Perez, A. C., Karst, J. C., Davi, M., Guijarro, J. I., Ladant, D., and Chenal, A. (2010) Characterization of the regions involved in the calcium-induced folding of the intrinsically disordered RTX motifs from the bordetella pertussis adenylate cyclase toxin. *Journal of molecular biology* **397**, 534-549
57. Karst, J. C., Sotomayor Perez, A. C., Guijarro, J. I., Raynal, B., Chenal, A., and Ladant, D. (2010) Calmodulin-induced conformational and hydrodynamic changes in the catalytic domain of Bordetella pertussis adenylate cyclase toxin. *Biochemistry* **49**, 318-328
58. Louis-Jeune, C., Andrade-Navarro, M. A., and Perez-Iratxeta, C. (2011) Prediction of protein secondary structure from circular dichroism using theoretically derived spectra. *Proteins*
59. Geourjon, C., and Deleage, G. (1995) SOPMA: significant improvements in protein secondary structure prediction by consensus prediction from multiple alignments. *Comput Appl Biosci* **11**, 681-684
60. Sotomayor-Perez, A. C., Karst, J. C., Ladant, D., and Chenal, A. (2012) Mean net charge of intrinsically disordered proteins: experimental determination of protein valence by electrophoretic mobility measurements. *Methods in molecular biology* **896**, 331-349
61. Karst, J. C., Sotomayor-Perez, A. C., Ladant, D., and Chenal, A. (2012) Estimation of intrinsically disordered protein shape and time-averaged apparent hydration in native conditions by a combination of hydrodynamic methods. *Methods in molecular biology* **896**, 163-177
62. Uversky, V. N. (2002) What does it mean to be natively unfolded? *European journal of biochemistry / FEBS* **269**, 2-12
63. Sebo, P., Glaser, P., Sakamoto, H., and Ullmann, A. (1991) High-level synthesis of active adenylate cyclase toxin of Bordetella pertussis in a reconstructed Escherichia coli system. *Gene* **104**, 19-24
64. Saron, M. F., Fayolle, C., Sebo, P., Ladant, D., Ullmann, A., and Leclerc, C. (1997) Anti-viral protection conferred by recombinant adenylate cyclase toxins from Bordetella pertussis carrying a CD8+ T cell epitope from lymphocytic choriomeningitis virus. *Proc Natl Acad Sci U S A* **94**, 3314-3319
65. Dadaglio, G., Morel, S., Bauche, C., Moukrim, Z., Lemonnier, F. A., Van Den Eynde, B. J., Ladant, D., and Leclerc, C. (2003) Recombinant adenylate cyclase toxin of Bordetella pertussis induces cytotoxic T lymphocyte responses against HLA\*0201-restricted melanoma epitopes. *Int Immunol* **15**, 1423-1430
66. Preville, X., Ladant, D., Timmerman, B., and Leclerc, C. (2005) Eradication of established tumors by vaccination with recombinant Bordetella pertussis adenylate cyclase carrying the human papillomavirus 16 E7 oncoprotein. *Cancer Res* **65**, 641-649
67. Uversky, V. N., Gillespie, J. R., and Fink, A. L. (2000) Why are "natively unfolded" proteins unstructured under physiologic conditions? *Proteins* **41**, 415-427

68. Gray, M. C., Donato, G. M., Jones, F. R., Kim, T., and Hewlett, E. L. (2004) Newly secreted adenylate cyclase toxin is responsible for intoxication of target cells by *Bordetella pertussis*. *Molecular microbiology* **53**, 1709-1719
69. Welch, R. A. (1991) Pore-forming cytolysins of gram-negative bacteria. *Molecular microbiology* **5**, 521-528
70. Herlax, V., and Bakas, L. (2007) Fatty acids covalently bound to alpha-hemolysin of *Escherichia coli* are involved in the molten globule conformation: implication of disordered regions in binding promiscuity. *Biochemistry* **46**, 5177-5184

## Figure legends

**Figure 1: Domain organization and structural disorder propensity of CyaA.** A) Schematic representation of CyaA localizing the catalytic domain (ACD), the translocation region (T), the hydrophobic region (HR), the acylation region (AR) and the cell-receptor binding domain (RD). Structural disorder propensity of CyaA analyzed by (B) FoldIndex, (C) IUPred and (D) GlobPlot.

**Figure 2: CyaA refolding followed by fluorescence and circular dichroism.** Refolding of urea-denatured apo-CyaA (open circles) or holo-CyaA (black circles) followed by (A) tryptophan intrinsic fluorescence, (B) ANS fluorescence and (C and D) CD in the far-UV region. Maximum emission wavelength values are reported for both tryptophan and ANS fluorescence. (C) Far-UV CD spectra of CyaA (1  $\mu$ M) in the absence (dashed line) and in the presence (full line) of 2 mM calcium are shown in the presence of 6 M urea and after extensive dialysis against buffer A or buffer B. Changes of mean residual ellipticity (MRE) of the  $n-\pi^*$  band followed at 220 nm are shown in panel D. For all spectra and MRE changes, the contributions from the buffer were subtracted.

**Figure 3: Size exclusion chromatography of CyaA in the presence and in the absence of urea after dialysis or desalting.** (A-B): Size exclusion chromatography (SEC) of CyaA on TSK 4000SWxl column equilibrated in 4 M urea in buffer A (without calcium) with the molecular mass (A) and hydrodynamic radius (B) distributions measured by tetra detector array (TDA). (C - F): SEC analysis on the TSK 4000SWxl column of CyaA samples after dialysis on Float-A-Lyzer G2 against buffer A (panel C) or buffer B (panel D), or after CyaA desalting on G25SF in buffer A (panel E) or buffer B (panel F).

**Figure 4: Analytical ultracentrifugation of CyaA after urea removal by desalting on G25.** CyaA (in 8 M urea) was chromatographed on G25SF equilibrated in buffer A or buffer B. The sedimentation distribution profile of CyaA (1.4  $\mu$ M) was analyzed with a Beckman-Coulter XL-I analytical ultracentrifuge using an AnTi rotor. Experimental data of sedimentation velocity (dots) in the absence (A) and in the presence (C) of 2 mM calcium were fitted with the Lamm equation (lines) and the distributions of the residual values are shown in panel (B) and (D) respectively. (E) Sedimentation coefficient distribution of apo-CyaA (dashed line), and holo-CyaA (thick line) deduced from the fitted curves.

**Figure 5: Refolding of CyaA into monomeric species by SEC-TDA.** (A) SEC-TDA analysis of CyaA (5  $\mu$ M in 8M urea) directly injected on a on TSK 4000SWxl column equilibrated in buffer B (with 2mM calcium). Black line: UV profile; red line: molecular mass. (B) SEC-TDA in same conditions of CyaA (in 8M urea) loaded at the following concentrations: 1 $\mu$ M: blue; 2.5 $\mu$ M: green; 5 $\mu$ M: red; 12 $\mu$ M: black. (C) The UV profiles shown in B are normalized to the monomer peak ( $\approx$ 14 mL) intensity to highlight the concentration-dependent distribution of monomers and multimers.

**Figure 6: Molecular confinement favors CyaA folding into monomeric species.** (A) SEC of CyaA on TSK 4000SWxl (particle size: 8  $\mu$ m) after urea removal by dialysis (dashed), desalting on G25SF (thin grey) and direct refolding on TSK 4000SWxl (bold trace). (B) SEC of CyaA on Superdex200 10/300 after urea removal by dialysis (dashed) and by direct refolding (bold trace) on the column. (C) SEC of CyaA directly loaded on Superdex200 10/300 (bold trace; particle size:  $11 \pm 2$   $\mu$ m) or on Sephacryl S200 (dashed trace; particle size:  $50 \pm 25$   $\mu$ m). Both columns had a bed volume of 24 mL. The O and M arrows indicate the oligomeric and monomeric fractions collected on the Superdex200 10/300 chromatography. (D) SEC of CyaA loaded on Superose 6HR (particle size:  $13 \pm 2$   $\mu$ m; total volume of 24 ml). Samples of 200  $\mu$ L of 5  $\mu$ M CyaA in 8 M urea, 20 mM Hepes, pH 7.4 were loaded in all experiments of direct refolding on column. All SEC were carried out in buffer B.

**Figure 7: Post-translational acylation of CyaA and calcium binding are required to produce CyaA monomers.** SEC of CyaA (A) and proCyaA (B) refolded on Superdex S200 5/150 in the absence (dashed traces, buffer A) and in the presence (thick traces, buffer B) of 2 mM calcium. Samples of 50  $\mu\text{L}$  of 5  $\mu\text{M}$  CyaA or proCyaA (in 8 M urea, 20 mM Hepes, pH 7.4) were loaded in each experiment.

**Figure 8: Circular dichroism and tryptophan quenching of CyaA.** A) Far-UV SR-CD spectrum of holo-CyaA monomers in buffer B. Deconvolution by K2D3 provides the following secondary structure content estimation: 24% of helix and 27% of beta-sheets. Inset: comparison between far-UV CD spectra of the monomeric (full line) and multimeric (dashed line) forms of CyaA acquired on an Aviv spectropolarimeter, showing that  $n-\pi^*$  bands of both species exhibit similar intensities. B) Near-UV CD of the urea-unfolded (dashed), multimeric (dotted) and monomeric (bold) CyaA. Row data (C) and Stern-Volmer analysis (D) of KI quenching of intrinsic tryptophan fluorescence of L-Trp (crosses), monomeric (black circles) and multimeric (open circles) CyaA species.

**Figure 9: Hemolytic and cAMP-inducing activities of the various CyaA preparations.** The different CyaA samples, i.e., CyaA renatured by G25 buffer exchange in the presence of calcium (black diamond), CyaA renatured by G25 buffer exchange in the absence of calcium (open diamond), the oligomeric (black square) and monomeric (black circle) CyaA species collected after refolding on TSK column in the presence of calcium (see O and M fractions in Figure 5C), were directly diluted into erythrocytes suspension ( $5 \times 10^8$  cells /ml in buffer B) to reach the indicated final concentrations. All hemolysis and cAMP production experiments were performed in the presence of 2 mM calcium, excepted the G25 buffer exchanged-CyaA in the absence of calcium that was tested in the presence of 4 mM EDTA. The hemolytic activity and intracellular cAMP accumulation were determined as described in experimental procedures.

TABLE 1

Comparison of expected and measured hydrodynamic radii.

Hydrodynamic radius values of CyaA were measured in 6M urea, 20 mM Hepes, pH 7.4 and in the monomeric state in 20 mM Hepes, 150 mM NaCl, 2 mM CaCl<sub>2</sub>, pH 7.4. The data were compared to the expected values for a protein of 177 kDa in various folding states. The relations from molecular masses and folding states and hydrodynamic radii were taken from (62). The  $R_H$  of the monomeric state of CyaA fits to a molten globule state. Several hypotheses may explain this observation: (i) some regions might be partially folded in the folded monomer; (ii) CyaA is a multidomain protein and could hence increase its friction with the solvent; (iii) the molecular shape of the monomeric CyaA is far from a spherical shape. All hypotheses are not mutually exclusive.

State of the protein	$R_H$ of a 177 kDa protein, nm	$R_H$ of CyaA, nm
Native	4.7	
Molten Globule	5	
Monomeric CyaA		$5.2 \pm 0.3$
Pre Molten Globule	7	
Natively Unfolded	10.9	
CyaA unfolded in 6M urea		$12 \pm 2$
Unfolded in UREA	12.2	
Unfolded in Guanidinium	13.4	

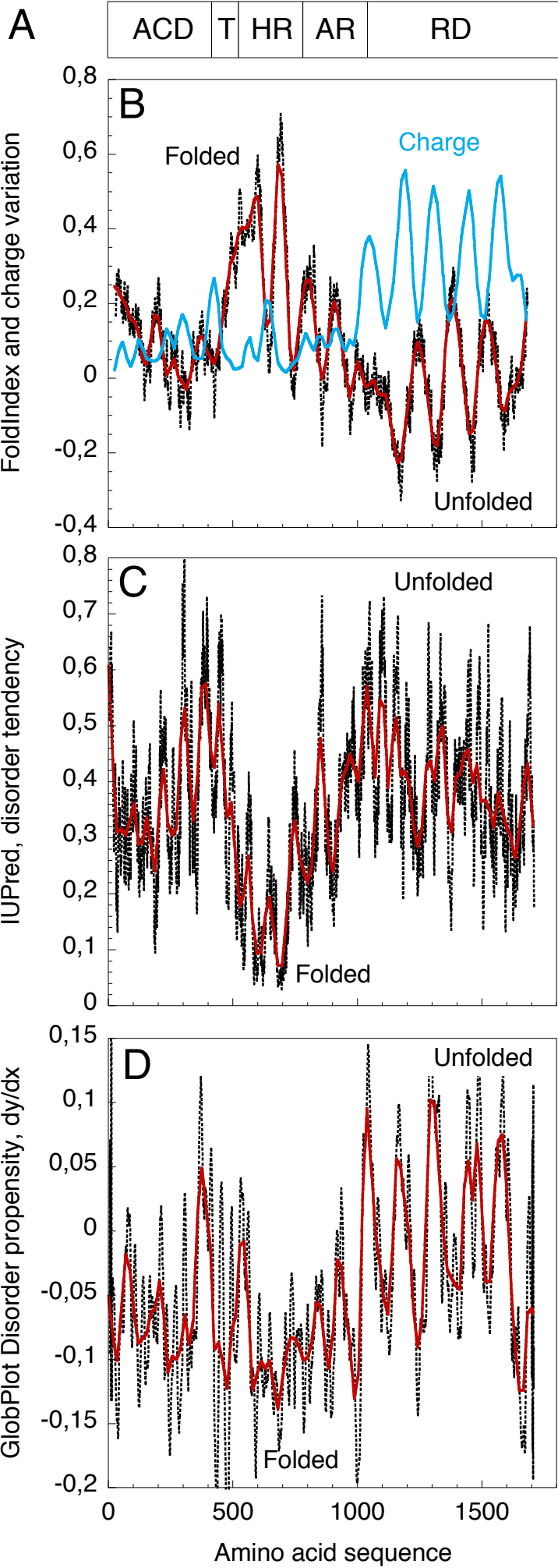


Figure 1

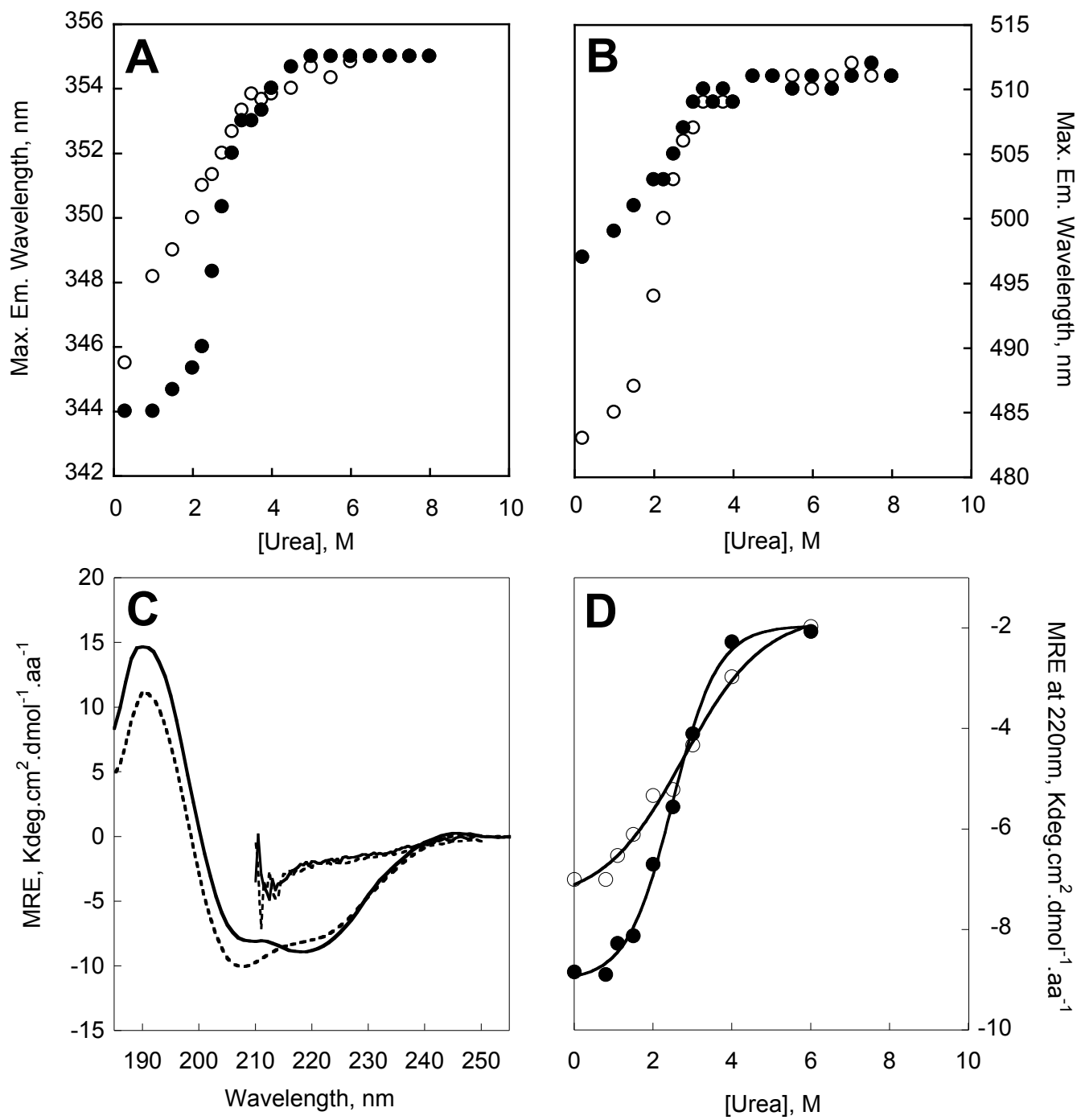


Figure 2

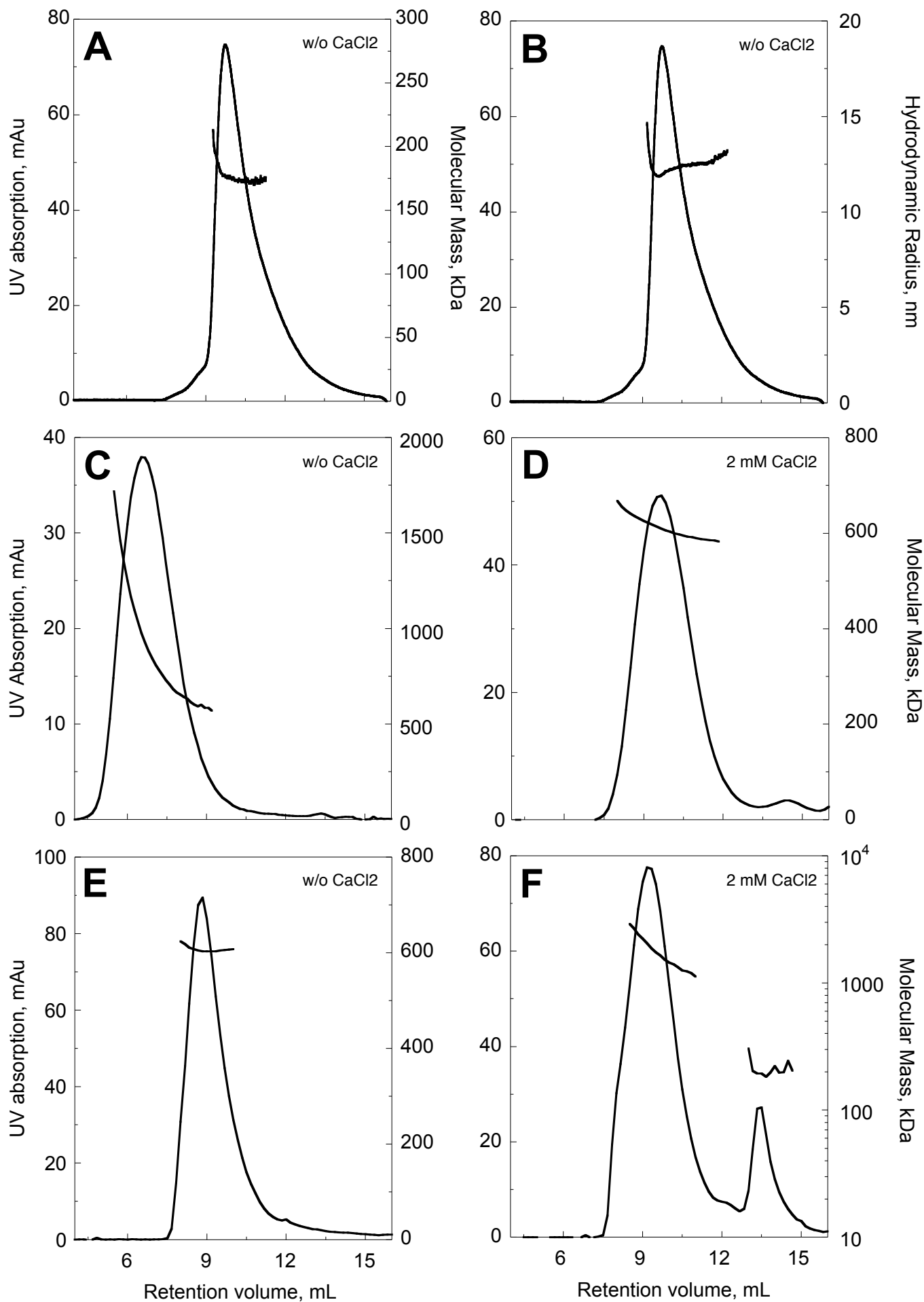


Figure 3

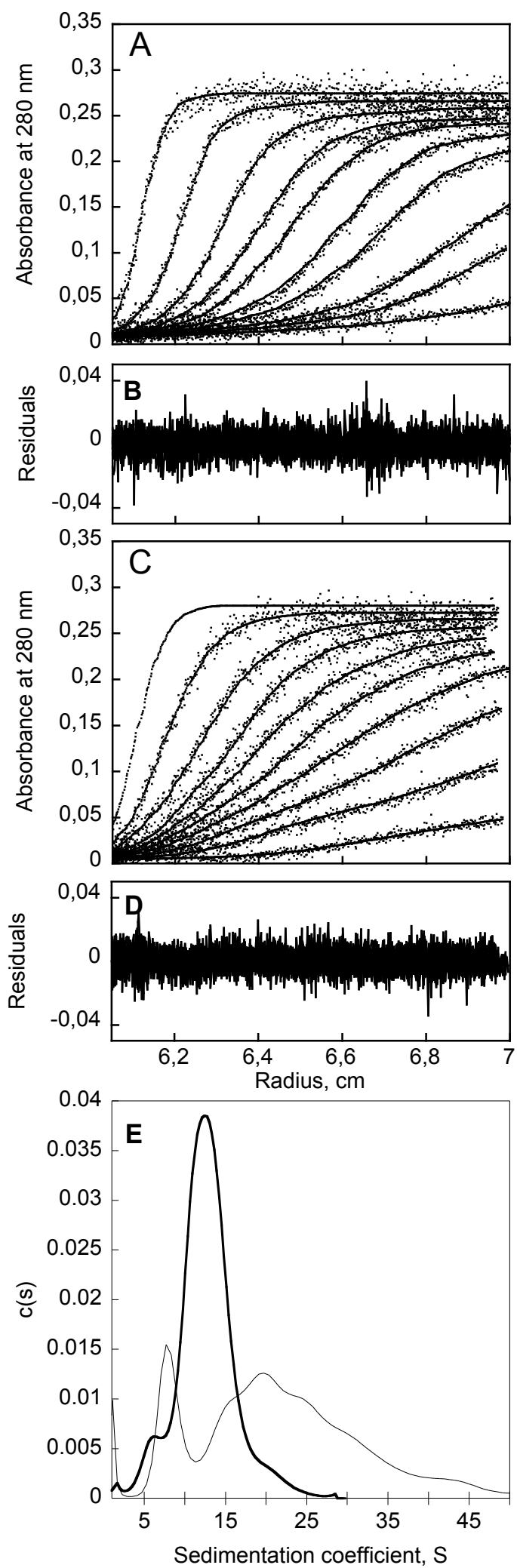


Figure 4

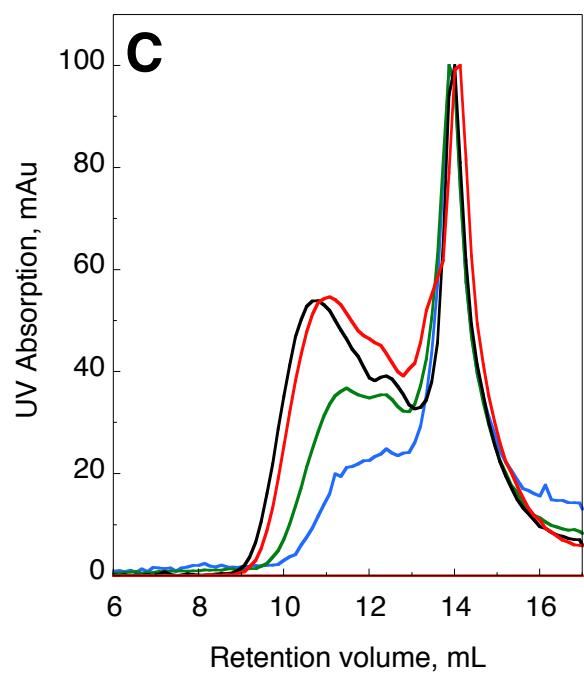
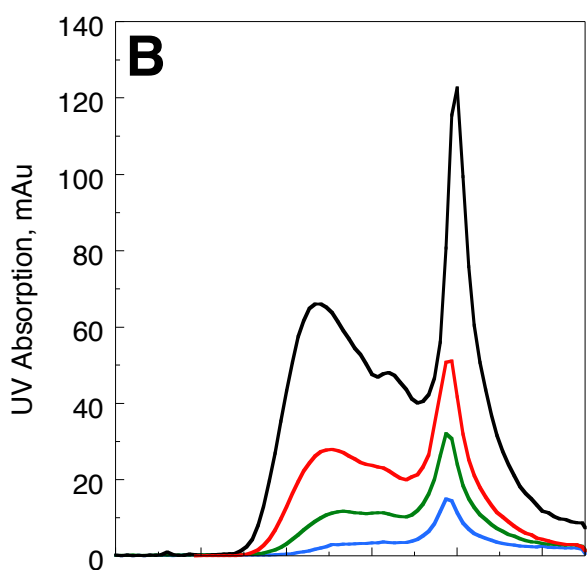
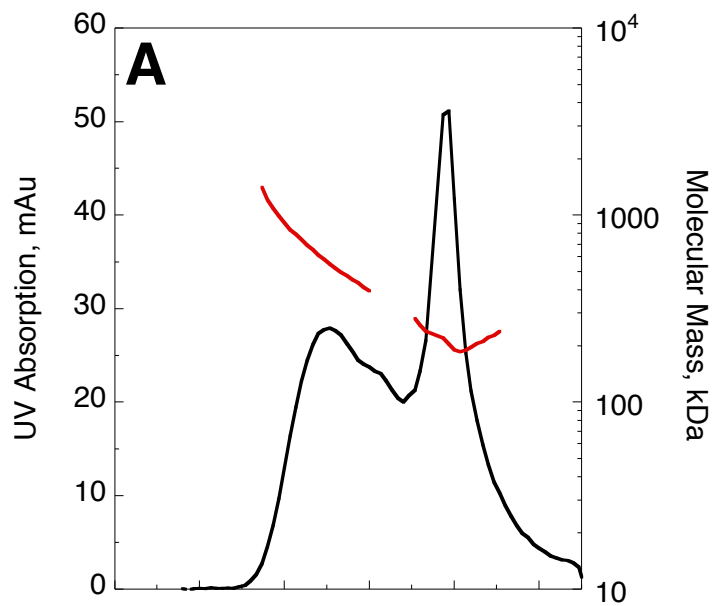


Figure 5

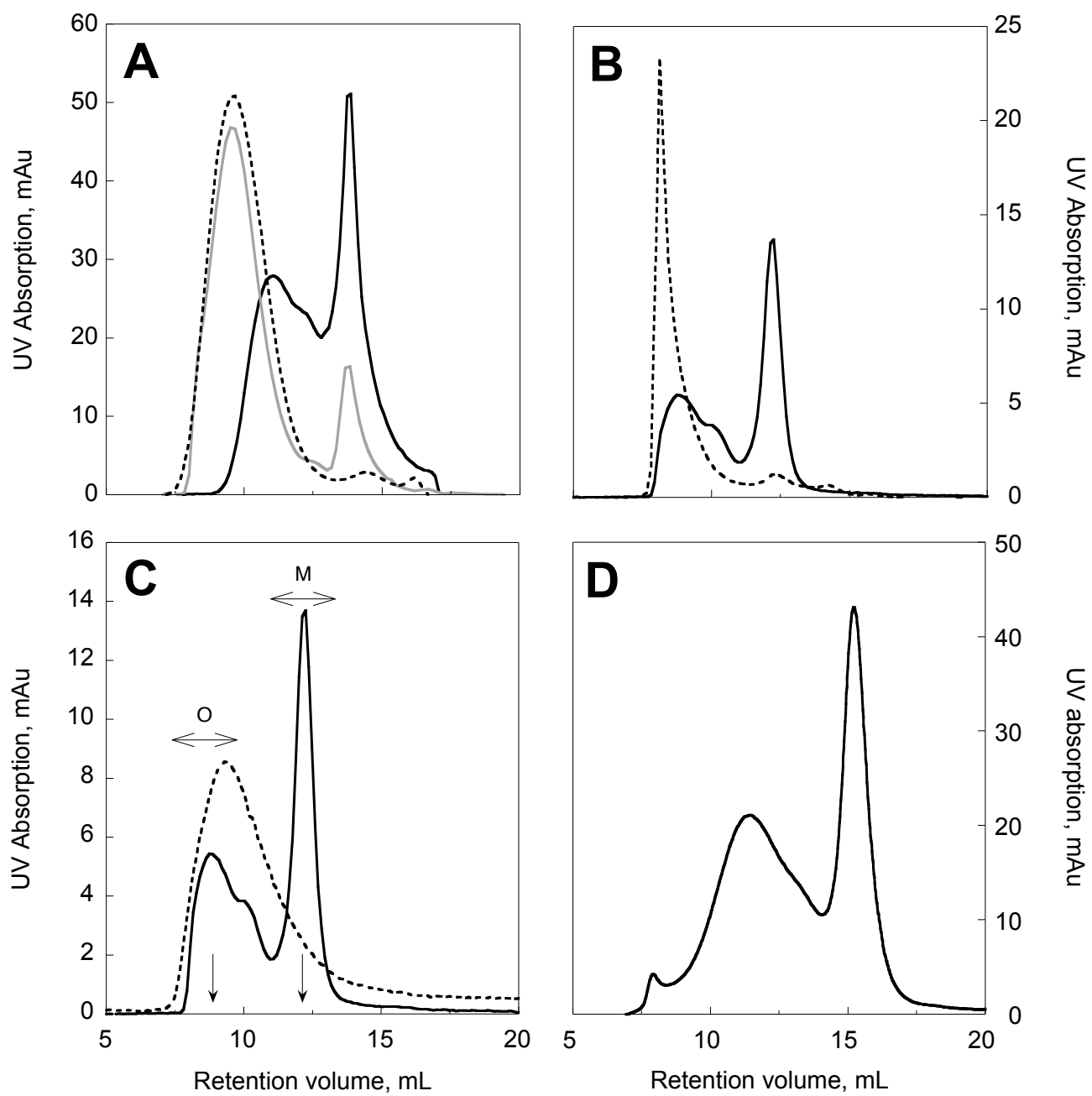


Figure 6

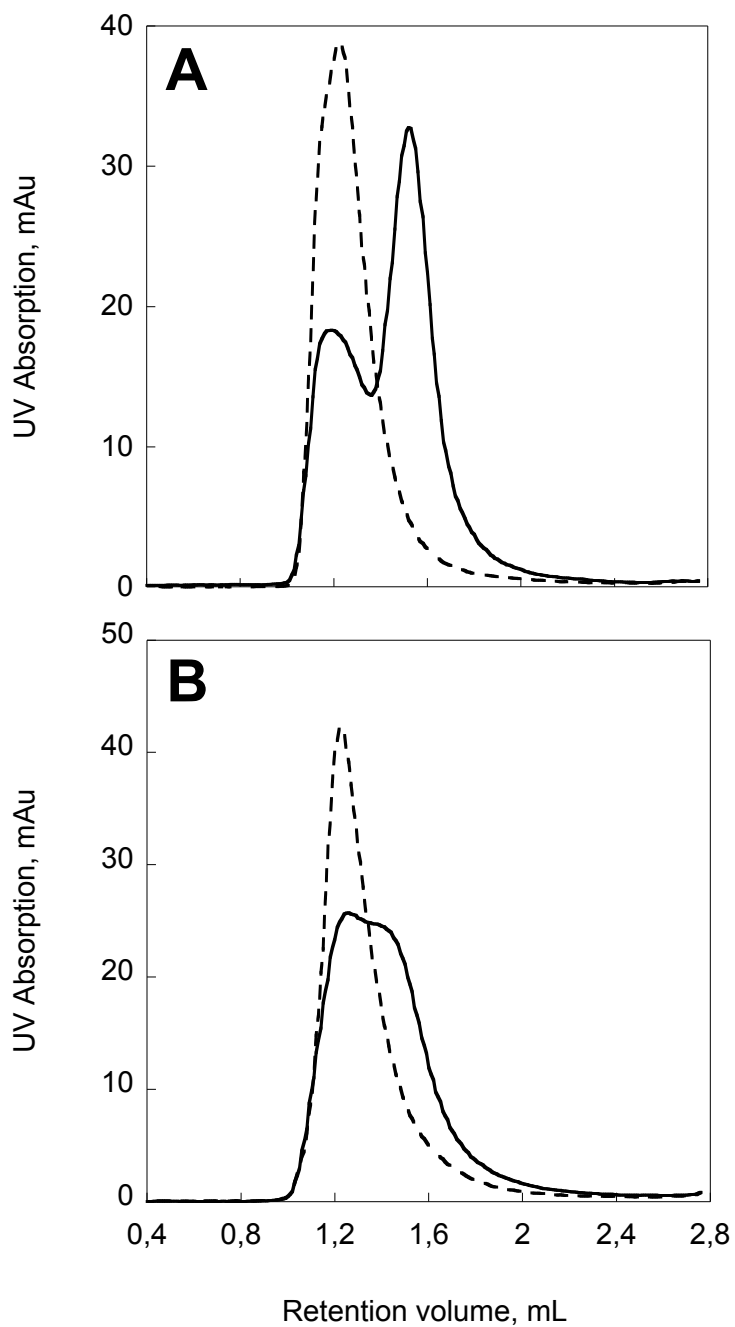


Figure 7

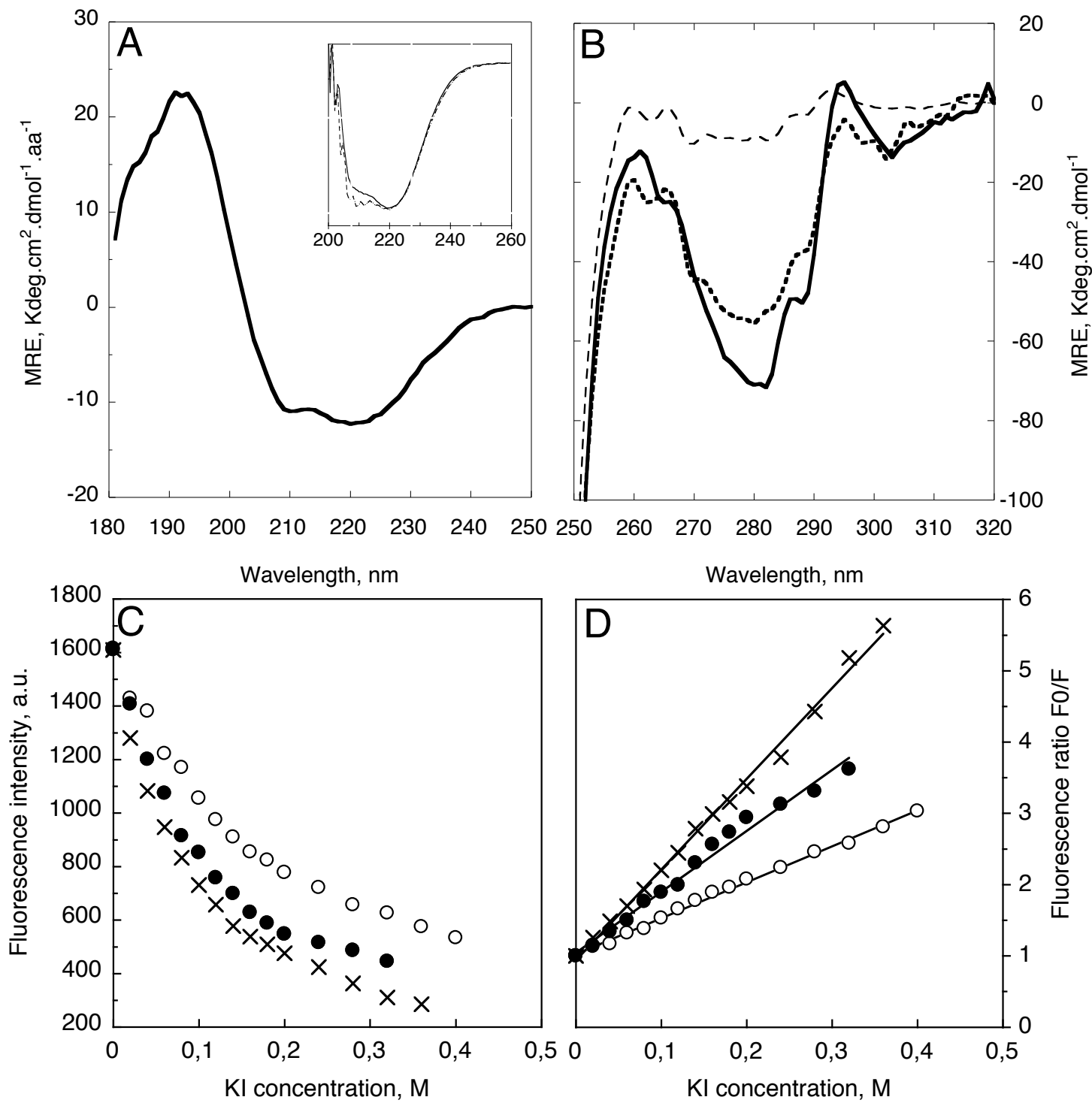


Figure 8

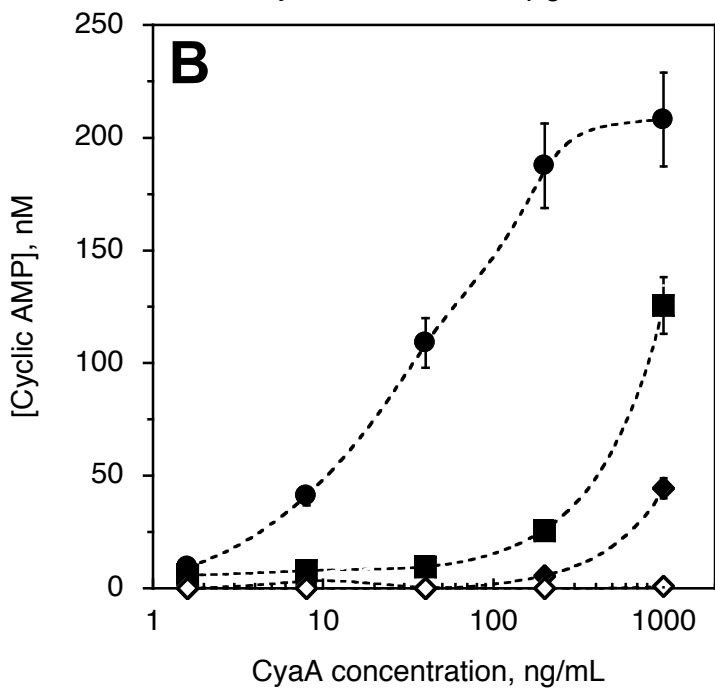
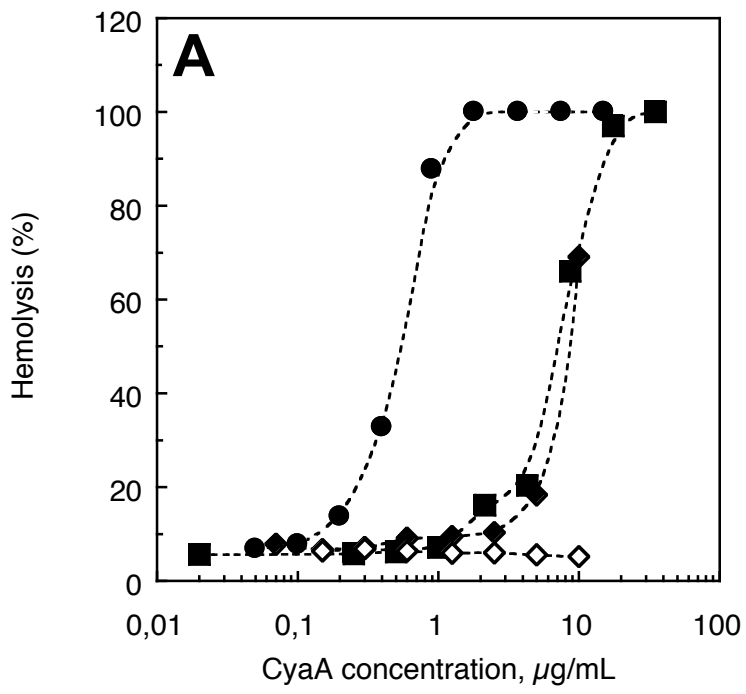


Figure 9